Arabian Journal of Chemistry (2022) **15**, 103682

King Saud University

Arabian Journal of Chemistry

www.ksu.edu.sa
www.sciencedirect.com

ORIGINAL ARTICLE

Design, synthesis, antimicrobial evaluations and *in silico* studies of novel pyrazol-5(4*H*)-one and 1*H*-pyrazol-5-ol derivatives

Em Canh Pham [a,*], Tuong Vi Le Thi [b,1], Long Tieu Phan [c,2], Huong-Giang T. Nguyen [c,2], Khanh N.B. Le [c,2], Tuyen Ngoc Truong [c,*]

[a] *Department of Medicinal Chemistry, Faculty of Pharmacy, Hong Bang International University, 700000 Ho Chi Minh City, Viet Nam*
[b] *Department of Pharmacology - Clinical Pharmacy, Faculty of Pharmacy, City Children's Hospital, 700000 Ho Chi Minh City, Viet Nam*
[c] *Department of Organic Chemistry, Faculty of Pharmacy, University of Medicine and Pharmacy at Ho Chi Minh City, 700000 Ho Chi Minh City, Viet Nam*

Received 23 October 2021; accepted 30 December 2021
Available online 5 January 2022

KEYWORDS

Pyrazolone;
Pyrazolol;
Antimicrobial;
ADMET parameters;
Molecular docking

Abstract A new series of 1,4-disubstituted 3-methylpyrazol-5(4*H*)-one derivatives were synthesized by reacting various substituted aromatic aldehydes with 3-methylpyrazol-5(4*H*)-one derivatives through Knoevenagel condensation by conventional as well as by exposure to microwave irradiations. After that newly synthesized compounds of 1,4-disubstituted 3-methyl-1*H*-pyrazol-5-ol were prepared from these derivatives by reduction reaction of sodium borohydride at 0–5 °C. Sixty-four heterocyclic compounds containing a pyrazole moiety were synthesized with good to excellent yields (51 to 91%). Compounds (**3d**, **3m**, **4a**, **4b**, **4d**, and **4g**) showed potent antibacterial activity against MSSA (Methicillin-susceptible strains of *Staphylococcus aureus*) and MRSA (Methicillin-resistant strains of *Staphylococcus aureus*) with MIC (the minimum inhibitory concentration) ranging between 4 and 16 μg/mL as compared to ciprofloxacin (MIC = 8–16 μg/mL). Compounds (**4a**, **4h**, **4i**, and **4l**) showed potent antifungal activity against Aspergillus niger with MIC ranging between 16 and 32 μg/mL as compared to fluconazole (MIC = 128 μg/mL). In

* Corresponding authors at: 120 Hoa Binh, Tan Phu District, Ho Chi Minh City 700000, Viet Nam. (E.C. Pham). 41 Dinh Tien Hoang, District 1, Ho Chi Minh City 700000, Viet Nam (T.N. Truong).
E-mail addresses: canhem112009@gmail.com (E.C. Pham), huonggiang@ump.edu.vn (H.-G.T. Nguyen), lnbkhanh@ump.edu.vn (K.N.B. Le), truongtuyen@ump.edu.vn (T.N. Truong).
[1] Postal address: 15 Vo Tran Chi, Binh Chanh District, Ho Chi Minh City 700000, Viet Nam.
[2] Postal address: 41 Dinh Tien Hoang, District 1, Ho Chi Minh City 700000, Viet Nam.
Peer review under responsibility of King Saud University.

Production and hosting by Elsevier

https://doi.org/10.1016/j.arabjc.2021.103682

particular, compound **4a** exhibited the strongest activity among the synthesized compounds in both bacterial and fungal strains with MIC ranging between 4 and 16 μg/mL. Furthermore, the nine most active compounds showed a good ADMET (absorption, distribution, metabolism, excretion, and toxicity) profile in comparison to ciprofloxacin and fluconazole as reference drugs. Molecular docking predicted that DHFR (dihydrofolate reductase) protein from *Staphylococcus aureus* and NMT (*N*-myristoyl transferase) protein from *Candida albicans* are the most suitable targets for the antimicrobial activities of these potent compounds.

1. Introduction

Heterocyclic compounds, as the most important organic compounds, are common pharmacophores with a wide range of biological activities which are arranged to deliver potent and selective drugs (Buu Hue et al., 2016; Em et al., 2021; Galal et al., 2009; Priego et al., 2002). In addition, a large number of biologically active natural substances are heterocyclic compounds. Therefore, heterocyclic chemistry is of interest to a large community of pharmaceutical chemists (Chand et al., 2017; Goetz et al., 2015). Pyrazole, pyrazolone, and pyrazolol are a group of heterocyclic compounds having great importance because of their broad spectrum of biological activities and their wide-ranging use as synthetic tools (Fig. 1). Pyrazolone and pyrazolol are five-membered rings containing two adjacent nitrogens and a ketone or alcohol group in their structure.

Pyrazole is an indispensable nucleus of a number of biologically active natural products, especially alkaloids (Kumar et al., 2013). The pyrazole ring is present as the core in a variety of leading drugs like Celebrex, Viagra, Ionazlac, Rimonabant, and Difenamizole, etc. Pyrazole derivatives have shown significant biological activities, such as antimicrobial (Faidallah et al., 2011; Vijesh et al., 2013), analgesic (Gokulan et al., 2012; Venkat Ragavan et al., 2009), antidiabetic (Faidallah et al., 2011), antiviral (el-Sabbagh et al., 2009), anti-inflammatory (Alam et al., 2013) and anticancer activities (Li et al., 2012; Manojkumar et al., 2009). This has demonstrated that the pyrazole nucleus presents great potential and impetus in developing drugs with strong pharmacological activity.

Pyrazolones are a very important class of the pyrazole family, they are known for more than one century (Horton et al., 2003). Many other NSAIDs like phenylbutazone, oxyphenbutazone, aminophenazone, propyphenazone, etc. contain pyrazolone as the basic nucleus and are widely used as analgesic, antipyretic and anti-inflammatory drugs. Compounds containing pyrazolone as parent scaffold is known to have a wide variety of therapeutic applications. These compounds are used as starting materials for the synthesis of various biologically active compounds. Pyrazolone derivatives exhibit remarkable antimicrobial (Bondock et al., 2008; Güniz Küçükgüzel et al., 2000; Sayed et al., 2018; Scuri et al., 2019), anti-inflammatory (Bekhit et al., 2005; Khode et al., 2009), analgesic (Amir et al., 2008), antidepressant (Abdel-Aziz et al., 2009), antihyperlipidemic (Idrees et al., 2009), antiviral (Makhija et al., 2004; Ouyang et al., 2008), anti-tuberculosis (Xu et al., 2017), antioxidant (Mariappan et al., 2010), anticancer (Park et al., 2005; Thomas et al., 2019). Due to their easier preparation and widely biological activity, the pyrazolone framework plays an essential role and represents an interesting template for combinatorial and medicinal chemistry.

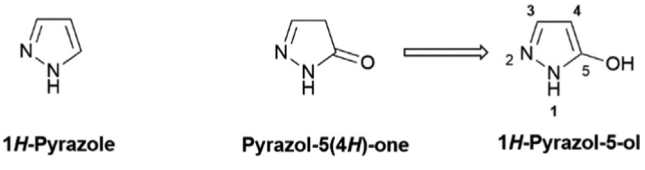

Fig. 1 The structure of pyrazole, pyrazol-5(4*H*)-one and pyrazol-5-ol.

Rationale and structure-based design as antimicrobial agents: Structure-activity relationship studies of pyrazolone ring system revealed in various kinds of literature (Clark et al., 2004; Sujatha et al., 2009), suggest the N-1, C-3, C-4 positions are very much important for structure–activity studies, in particular, the C-3 position can increase chemotherapeutic activity when attached to different heterocyclic rings. Since *N*-substitutions in pyrazolone exhibit biologically active compounds (Kimata et al., 2007), we were interested in designing compounds containing them (Fig. 2). Our designed derivatives and antimicrobial drugs Sulfaphenazole, OSU-03012, and derivatives of Menozzi et al., 2004 share three common essential structural features i) A planar pyrazole moiety. ii) Aromatic ring at position N1. iii) Aromatic ring with different substituted at other position (3 or 4). Moreover, different positions of a nitro group, aromatic moieties substituted with different hydrophobic or hydrophilic substituents, and the conversion of pyrazolone to pyrazolol were designed in order to examine their effects on antimicrobial activity.

The molecular docking approach is a type of bioinformatic model that involves protein–ligand interaction at the atomic level. This interaction is comparable to the lock-and-key principle, which has been used to discover target structures for the active sites of proteins as well as to elucidate the potential mechanism of action. On the other hand, ligands can bind with proteins through various types of interactions, mainly hydrogen bonding, hydrophobic bonding, van der Waals forces, and salt bridges, and are characterized by binding affinity (Em et al., 2021).

The development of antibiotic resistance in microorganisms, as well as economic incentives, has resulted in research and development in search of new antibiotics to maintain an effective drug supply at all times. It is important to find out newer, safer, and more effective antibiotics with a broad spectrum of activity. Although several antifungal agents and the azole class of drugs are currently available there is clearly a critical need for the development of new specific antimicrobial agents. Therefore, the purpose of this study is to synthesize novel 3-methylpyrazol-5(4*H*)-one and 3-methyl-1*H*-pyrazol-5-ol derivatives with various substituted aryl at positions 1 and 4, and evaluation of their antibacterial and antifungal activities. The synthesized derivatives will be investigated *in silico* to understand the potential for drug-receptor interaction.

2. Results and discussion

2.1. Chemistry

The phenylhydrazine derivatives with a 3-nitro or 4-nitro group are the starting material for the preparation of 3-methylpyrazol-5(4*H*)-one and 3-methyl-1*H*-pyrazol-5-ol derivatives. The process of synthetic research consists of three steps (Scheme 1). Firstly, 1-monosubstituted 3-methylpyrazol-5(4*H*)-one derivatives (**1a-1b**) were synthesized via the

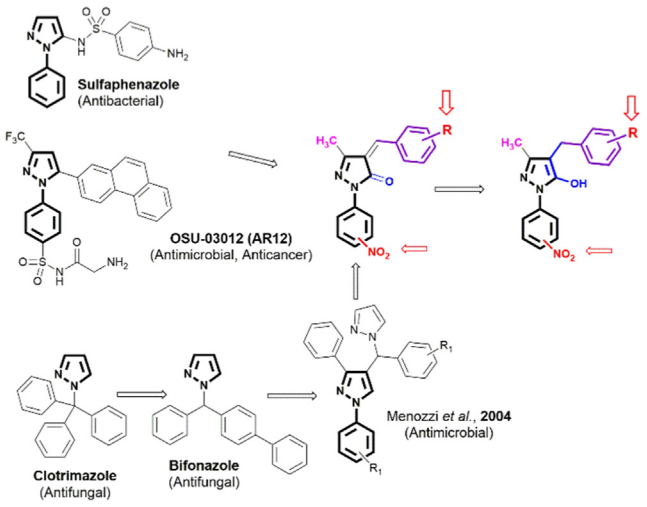

Fig. 2 Rational study design, illustrating the structure of the newly designed pyrazol-5(4*H*)-one and 1*H*-pyrazol-5-ol derivatives with representative examples for antimicrobial drugs.

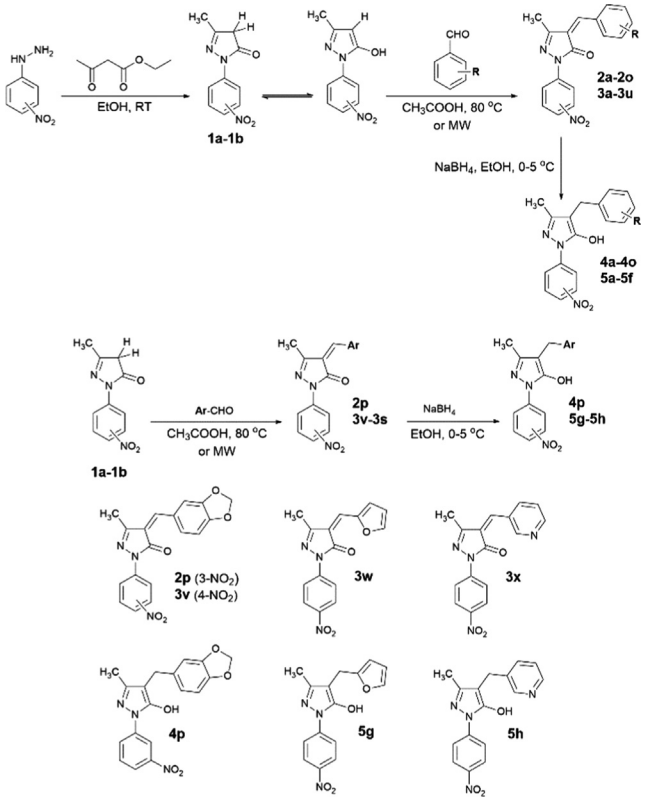

Scheme 1 Construction of 1,4-disubstituted 3-methylpyrazol-5(4*H*)-one and 3-methyl-1*H*-pyrazol-5-ol derivatives (*MW: microwave irradiation*).

acid-catalyzed condensation reaction of phenylhydrazines and ethyl acetoacetate (Ramajayam et al., 2010; Sehout et al., 2021). Secondly, a series of 1,4-disubstituted 3-methylpyrazol-5(4*H*)-one derivatives (**2a-2p**, **3a-3x**) have been synthesized by condensing pyrazol-5(4*H*)-one (**1a-1b**) with substituted aromatic aldehydes using conventional heating and microwave-assisted synthesis. The reaction time has been dramatically reduced, as using conventional heating the reaction is carried out in 3 h compared with 10 min heating in the microwave. Furthermore, the reaction yield has increased ranging between 6 and 7% with microwave assistance. Finally, a series of 1,4-disubstituted 3-methyl-1*H*-pyrazol-5-ol derivatives (**4a-4p**, **5a-5h**) were prepared from 1,4-disubstituted 3-methylpyrazol-5(4*H*)-one derivatives respectively by reduction reaction of sodium borohydride at 0–5 °C. Sixty-four derivatives have been synthesized in good to excellent yields (51 to 91%) (Tables 1 and 2). All compounds have physical–chemical properties of fragments (MW < 500) or lead-like (MW < 350) that follow Lipinski's rules which could lead to potent compounds for further development (Congreve et al., 2003; Lipinski, 2004). Especially, forty-five derivatives (**2a-2j**, **2l**, **2n-2o**, **3c**, **3e**, **3j-3k**, **3m**, **3o**, **3r**, **3u**, **3x**, **4a-4p**, **5a-5f**, and **5h**) are new compounds.

The IR spectra of compounds **2** and **3** displayed two strong absorbance bands in the ν 1530–1505 and 1350–1325 cm^{-1} regions which are distinctive of the NO_2 group as well as a strong absorbance band in the ν 1750–1650 cm^{-1} region characteristic of carbonyl (C═O) of pyrazol-5(4*H*)-one derivatives. However, IR of compounds **4** and **5** revealed the disappearance of band distinctive of the carbonyl group due to the conversion to the hydroxy group (C─OH) of 1*H*-pyrazol-5-ol derivatives. In addition, ^{1}H NMR spectra of compounds **4** and **5** indicated the characteristic OH protons as a broad singlet in the δ 11.50–10.50 ppm region, as well as the distinctive singlet for ─CH_2─Ar proton in the δ 3.80–3.30 ppm region. In contrast, ^{1}H NMR spectra of compounds **2** and **3** did not show two types of these proton signals but revealed the appearance of a singlet in the 8.10–7.60 ppm region of the ═CH─Ar group. Furthermore, the C═O group was identified at δ 165.0–153.0 ppm in the ^{13}C NMR spectrum of compounds **2** and **3.** The molecular ion peak M (*m*/*z*) of compounds **2**–**5** was observed in the mass spectrum, confirming the hypothesized structure.

2.2. In vitro antibacterial and antifungal activities

Antimicrobial activities (exhibited by MIC values) including antibacterial activities at two strains of Gram-negative (EC - *Escherichia coli* and PA - *Pseudomonas aeruginosa*) and three strains of Gram-positive (SF - *Streptococcus faecalis*, MSSA, MRSA) and antifungal activities (CA - *Candida albicans* and AN - *Aspergillus niger*) of all synthesized compounds are summarized in Table 3. With antimicrobial activities of series of 3- and 4-nitro-3-methyl-1*H*-pyrazol-5(4*H*)-one, compounds **2a-2b, 3a, 3c, 3f-3k, 3n-3o, 3q-3r** and **3w-3x** are totally inactive at 5 strains of bacteria and 2 strains of fungi (MIC > 1024 μg/mL). Compounds **3b**, **3e**, **3l**, **3p**, and **3s-3v** are totally inactive at 3 strains of bacteria (EC, PA, SF) and 2 strains of fungi (CA, AN), but showed weak to moderate activities at the Gram-positive strains MSSA and MRSA (MIC 32–256 μg/mL). Among substituted arylidene compounds of 4-nitro-3-methyl-1*H*-pyrazol-5(4*H*)-one, **3d** (2,4-dichloro) and **3m** (3-hydroxy) showed good antibacterial activities against MSSA and MRSA with MIC ranging between 4 and 16 μg/mL as compared to ciprofloxacin (Cipro, MIC = 8–16 μg/mL). The compound **3m** showed significant and better activities against MSSA and MRSA than Cipro

Table 1 Yields and physicochemical parameters of **3-nitro** 3-methylpyrazol-5(4*H*)-one and 3-methyl-1*H*-pyrazol-5-ol derivatives (**2a-2p** and **4a-4p**).

Entry	R group	Code	Physicochemical parameters		Yield
1H-Pyrazol-5(4H)-one					
1	2-Cl	**2a**	MW: 341.7510 NHA: 3 NHD: 1	NRB: 3 LogP: 4.1250 PSA: 72.98	**77**
2	4-Cl	**2b**	MW: 341.7510 NHA: 3 NHD: 1	NRB: 3 LogP: 4.1250 PSA: 72.98	**78**
3	2-Cl, 6-F	**2c**	MW: 359.7414 NHA: 4 NHD: 1	NRB: 3 LogP: 4.2862 PSA: 72.98	**78**
4	3,4-Cl_2	**2d**	MW: 376.1930 NHA: 3 NHD: 1	NRB: 3 LogP: 4.7470 PSA: 72.98	**81**
5	2,4-$(OCH_3)_2$	**2e**	MW: 367.3610 NHA: 5 NHD: 1	NRB: 5 LogP: 3.3080 PSA: 91.44	**69**
6	3,4-$(OCH_3)_2$	**2f**	MW: 367.3610 NHA: 5 NHD: 1	NRB: 5 LogP: 3.0595 PSA: 91.44	**75**
7	4-F	**2g**	MW: 325.2994 NHA: 4 NHD: 1	NRB: 3 LogP: 3.6643 PSA: 72.98	**86**
8	2-OH	**2h**	MW: 323.3080 NHA: 4 NHD: 2	NRB: 3 LogP: 3.0940 PSA: 93.21	**74**
9	4-OH	**2i**	MW: 323.3080 NHA: 4 NHD: 2	NRB: 3 LogP: 3.0940 PSA: 93.21	**75**
10	3-OH, 4-OCH_3	**2j**	MW: 353.3340 NHA: 5 NHD: 2	NRB: 4 LogP: 2.9965 PSA: 102.44	**63**
11	4-OH, 3-OCH_3	**2k**	MW: 353.3340 NHA: 5 NHD: 2	NRB: 4 LogP: 2.9965 PSA: 102.44	**59**
12	3-OCH_3	**2l**	MW: 337.3350 NHA: 4 NHD: 1	NRB: 4 LogP: 3.4055 PSA: 82.21	**77**
13	4-OCH_3	**2m**	MW: 337.3350 NHA: 4 NHD: 1	NRB: 4 LogP: 3.4055 PSA: 82.21	**75**
14	4-SCH_3	**2n**	MW: 353.3960 NHA: 3 NHD: 1	NRB: 4 LogP: 4.2698 PSA: 72.98	**74**
15	3-NO_2	**2o**	MW: 352.3060 NHA: 4 NHD: 2	NRB: 4 LogP: 3.2654 PSA: 113.29	**85**
16		**2p**	MW: 351.3180 NHA: 5 NHD: 1	NRB: 3 LogP: 3.2541 PSA: 91.44	**80**
1H-Pyrazol-5-ol					
17	2-Cl	**4a**	MW: 343.7670 NHA: 4 NHD: 2	NRB: 4 LogP: 4.1920 PSA: 76.14	**84**
18	4-Cl	**4b**	MW: 343.7670 NHA: 4 NHD: 2	NRB: 4 LogP: 4.1920 PSA: 76.14	**82**
19	2-Cl, 6-F	**4c**	MW: 361.7574 NHA: 5 NHD: 2	NRB: 4 LogP: 4.3533 PSA: 76.14	**79**
20	3,4-Cl_2	**4d**	MW: 378.2090 NHA: 4 NHD: 2	NRB: 4 LogP: 4.8140 PSA: 76.14	**82**

Table 1 (*continued*)

Entry	R group	Code	Physicochemical parameters		Yield
21	2,4-$(OCH_3)_2$	**4e**	MW: 369.3770	NRB: 6	**84**
			NHA: 6	LogP: 3.3750	
			NHD: 2	PSA: 94.6	
22	3,4-$(OCH_3)_2$	**4f**	MW: 369.3770	NRB: 6	**81**
			NHA: 6	LogP: 3.1166	
			NHD: 2	PSA: 94.6	
23	4-F	**4g**	MW: 327.3154	NRB: 4	**87**
			NHA: 5	LogP: 3.7313	
			NHD: 2	PSA: 76.14	
24	2-OH	**4h**	MW: 325.3240	NRB: 4	**82**
			NHA: 5	LogP: 3.1611	
			NHD: 3	PSA: 93.37	
25	4-OH	**4i**	MW: 325.3240	NRB: 4	**77**
			NHA: 5	LogP: 3.1611	
			NHD: 3	PSA: 93.37	
26	3-OH, 4-OCH_3	**4j**	MW: 355.3500	NRB: 5	**84**
			NHA: 6	LogP: 3.0636	
			NHD: 3	PSA: 105.6	
27	4-OH, 3-OCH_3	**4k**	MW: 355.3500	NRB: 5	**87**
			NHA: 6	LogP: 3.0636	
			NHD: 3	PSA: 105.6	
28	3-OCH_3	**4l**	MW: 339.3510	NRB: 5	**85**
			NHA: 5	LogP: 3.4725	
			NHD: 2	PSA: 85.37	
29	4-OCH_3	**4m**	MW: 339.3510	NRB: 5	**81**
			NHA: 5	LogP: 3.4725	
			NHD: 2	PSA: 85.37	
30	4-SCH_3	**4n**	MW: 355.4120	NRB: 5	**81**
			NHA: 4	LogP: 4.3368	
			NHD: 2	PSA: 76.14	
31	3-NO_2	**4o**	MW: 354.3220	NRB: 5	**85**
			NHA: 5	LogP: 3.3324	
			NHD: 3	PSA: 116.45	
32		**4p**	MW: 353.3340	NRB: 4	**82**
			NHA: 6	LogP: 3.3211	
			NHD: 2	PSA: 94.6	

Yields of conventional heating method, MW: molecular weight, NHA: number of hydrogen bond acceptor, NHD: number of hydrogen bond donor, NRB: number rotatable bond, PSA: polar surface area (Angstroms squared).

with MIC 4 and 8 μg/mL, respectively. This suggests that the 4-nitro group of the aromatic ring at position 1 of the pyrazolone scaffold enhanced antibacterial activities against MSSA and MRSA strains.

With antimicrobial activities of series of 3- and 4-nitro-3-methyl-1*H*-pyrazol-5-ol, compounds **4c**, **4f**, **4j-4k**, **4m-4o**, and **5a-5h** showed weak to moderate activities at 4 strains of bacteria (EC, SF, MSSA, and MRSA) and 2 strains of fungi (CA, AN) with MIC > 64 μg/mL at fungi strain AN and ranging between 32 and 128 μg/mL at the bacteria strains. However, compounds **4a** (2-chloro), **4b** (4-chloro), **4d** (3,4-dichloro), and **4g** (4-fluoro) showed good antibacterial activities against the Gram-positive strains MSSA and MRSA with MIC ranging between 8 and 16 μg/mL as compared to Cipro (MIC = 8–16 μg/mL). On the other hand, compounds **4e** (2,4-dimethoxy) and **4p** (benzo[d][1,3]dioxol-5-yl group at position 4) showed good antibacterial activity against MSSA and EC, respectively with MIC value at 16 μg/mL. Compounds **4h** (2-hydroxy), **4i** (4-hydroxy), and **4l** (3-methoxy) showed weak to moderate activities at the Gram-negative and Gram-positive strains suggesting that these compounds are less potent to cross the Gram-negative and Gram-positive membrane to reach the target as compared to Cipro. In contrast, for antifungal activity, compounds **4h**, **4i** and **4l** displayed promising activity against *Aspergillus niger* with MIC value at 32 μg/mL as compared to Flu (MIC = 128 μg/mL). In particular, compound **4a** exhibited the strongest activity among the synthesized compounds in both bacterial and fungal strains with MIC ranging between 4 and 16 μg/mL as compared to Cipro and Flu, except for did not show antibacterial activity at Gram-negative strain PA. This suggests that pyrazolone is a less potent scaffold than pyrazolol for antibacterial and antifungal activities. From the structure–activity relationship (SAR), the presence of the chloro/ fluoro group in the aromatic ring at position 4 of 1-(3-nitrophenyl)-1*H*-pyrazol-5-ol scaffold is more desirable for enhanced antibacterial activity in **4a**, **4b**, **4d** and **4g**, and antifungal activity in **4a**.

In published studies, 1,3-disubstituted-1*H*-pyrazol-5-ol derivatives which are the analogs of known radical scavenger "edaravone" showed good radical scavenging capacity

Table 2 Yields and physicochemical parameters of **4-nitro** 3-methyl-1*H*-pyrazol-5(4*H*)-one and 3-methyl-1*H*-pyrazol-5-ol derivatives (**3a-3x** and **5a-5h**).

Entry	R group	Code	Physicochemical parameters		Yield
1	2-Cl	**3a**	MW: 341.7510	NRB: 3	**81**
			NHA: 3	LogP: 4.1250	
			NHD: 1	PSA: 72.98	
2	4-Cl	**3b**	MW: 341.7510	NRB: 3	**85**
			NHA: 3	LogP: 4.1250	
			NHD: 1	PSA: 72.98	
3	2-Cl, 6-F	**3c**	MW: 359.7414	NRB: 3	**84**
			NHA: 4	LogP: 4.2862	
			NHD: 1	PSA: 72.98	
4	2,4-Cl_2	**3d**	MW: 376.1930	NRB: 3	**75**
			NHA: 3	LogP: 4.7470	
			NHD: 1	PSA: 72.98	
5	3,4-Cl_2	**3e**	MW: 376.1930	NRB: 3	**75**
			NHA: 3	LogP: 4.7470	
			NHD: 1	PSA: 72.98	
6	2,4-$(OCH_3)_2$	**3f**	MW: 367.3610	NRB: 5	**85**
			NHA: 5	LogP: 3.3080	
			NHD: 1	PSA: 91.44	
7	2,5-$(OCH_3)_2$	**3g**	MW: 367.3610	NRB: 5	**86**
			NHA: 5	LogP: 3.3080	
			NHD: 1	PSA: 91.44	
8	3,4-$(OCH_3)_2$	**3h**	MW: 367.3610	NRB: 5	**80**
			NHA: 5	LogP: 3.0495	
			NHD: 1	PSA: 91.44	
9	4-$N(CH_3)_2$	**3i**	MW: 350.3780	NRB: 4	**80**
			NHA: 4	LogP: 3.7274	
			NHD: 1	PSA: 76.22	
10	4-OC_2H_5	**3j**	MW: 351.3620	NRB: 5	**85**
			NHA: 4	LogP: 3.8334	
			NHD: 1	PSA: 82.21	
11	3-OC_2H_5, 4-OH	**3k**	MW: 367.3610	NRB: 5	**51**
			NHA: 5	LogP: 3.4244	
			NHD: 2	PSA: 102.44	
12	4-F	**3l**	MW: 325.2994	NRB: 3	**86**
			NHA: 4	LogP: 3.6643	
			NHD: 1	PSA: 72.98	
13	3-OH	**3m**	MW: 323.3080	NRB: 3	**77**
			NHA: 4	LogP: 3.0940	
			NHD: 2	PSA: 93.21	
14	4-OH	**3n**	MW: 323.3080	NRB: 3	**78**
			NHA: 4	LogP: 3.0940	
			NHD: 2	PSA: 93.21	
15	3-OH, 4-OCH_3	**3o**	MW: 353.3340	NRB: 4	**57**
			NHA: 5	LogP: 2.9965	
			NHD: 2	PSA: 102.44	
16	3-OCH_3	**3p**	MW: 337.3350	NRB: 4	**71**
			NHA: 4	LogP: 3.4055	
			NHD: 1	PSA: 82.21	
17	4-OCH_3	**3q**	MW: 337.3350	NRB: 4	**75**
			NHA: 4	LogP: 3.4055	
			NHD: 1	PSA: 82.21	
18	4-SCH_3	**3r**	MW: 353.3960	NRB: 4	**80**
			NHA: 3	LogP: 4.2698	
			NHD: 1	PSA: 72.98	
19	3-NO_2	**3s**	MW: 352.3060	NRB: 4	**85**
			NHA: 4	LogP: 3.2654	
			NHD: 2	PSA: 113.29	
20	4-NO_2	**3t**	MW: 352.3060	NRB: 4	**65**
			NHA: 4	LogP: 3.2654	
			NHD: 2	PSA: 113.29	
21	2,4,5-$(OCH_3)_3$	**3u**	MW: 397.3870	NRB: 6	**82**
			NHA: 6	LogP: 2.9520	

Table 2 (*continued*)

Entry	R group	Code	Physicochemical parameters		Yield
			NHD: 1	PSA: 100.67	
22		**3v**	MW: 351.3180	NRB: 3	**80**
			NHA: 5	LogP: 3.2541	
			NHD: 1	PSA: 91.44	
23		**3w**	MW: 297.2700	NRB: 3	**84**
			NHA: 4	LogP: 2.1841	
			NHD: 1	PSA: 82.21	
24		**3x**	MW: 308.2970	NRB: 3	**79**
			NHA: 4	LogP: 2.2511	
			NHD: 1	PSA: 85.34	
25	2-Cl	**5a**	MW: 343.7670	NRB: 4	**91**
			NHA: 4	LogP: 4.1920	
			NHD: 2	PSA: 76.14	
26	2-Cl, 6-F	**5b**	MW: 361.7574	NRB: 4	**82**
			NHA: 5	LogP: 4.3533	
			NHD: 2	PSA: 76.14	
27	2,4-$(OCH_3)_2$	**5c**	MW: 369.3770	NRB: 6	**89**
			NHA: 6	LogP: 3.3750	
			NHD: 2	PSA: 94.6	
28	2,5-$(OCH_3)_2$	**5d**	MW: 369.3770	NRB: 6	**89**
			NHA: 6	LogP: 3.3750	
			NHD: 2	PSA: 94.6	
29	4-OCH_3	**5e**	MW: 339.3510	NRB: 5	**81**
			NHA: 5	LogP: 3.4725	
			NHD: 2	PSA: 85.37	
30	4-SCH_3	**5f**	MW: 355.4120	NRB: 5	**90**
			NHA: 4	LogP: 4.3368	
			NHD: 2	PSA: 76.14	
31		**5g**	MW: 299.2860	NRB: 4	**80**
			NHA: 5	LogP: 2.2298	
			NHD: 2	PSA: 85.37	
32		**5h**	MW: 310.3130	NRB: 4	**81**
			NHA: 5	LogP: 2.3181	
			NHD: 2	PSA: 88.5	

Yields of conventional heating method, MW: molecular weight, NHA: number of hydrogen bond acceptor, NHD: number of hydrogen bond donor, NRB: number rotatable bond, PSA: polar surface area (Angstroms squared).

(Sarojini et al., 2010). In addition, azo clubbed 1*H*-pyrazol-5-ol derivatives showed moderate antibacterial potential against Gram-negative strains with MIC value of 312.5 μg/mL, and good affinity with DNA (Chaitannya et al., 2019). Some 4,4′-(arylmethylene)bis-(3-methyl-1-phenyl-1*H*-pyrazol-5-ol) derivatives which contain thiophene ring or bearing —$N(CH_3)_2$, —OCH_3 and —Cl groups on the phenyl ring have shown excellent DPPH radical scavenging activity (EC_{50} 7.69–19.03 μg/mL), good anti-inflammatory activity (EC_{50} 10.87–12.25 μg/mL), and potent *in vitro* antimicrobial activity against bacterial strains *Escherichia coli*, *Staphylococcus aureus*, *Pseudomonas aeruginosa,* and *Micrococcus luteus* and fungal strains *Aspergillus niger*, and *Candida albicans* compared to ciprofloxacin, streptomycin, and fluconazole (Pravin et al., 2017). Some of our synthesized compounds exhibited more potential antimicrobial activity when compared with compounds of Chaitannya et al. (2019) and Pravin et al. (2017). This may be due to our compound structures that have added a nitro substituent (—NO_2) at position 3 or 4 on the phenyl ring of 1-phenyl-1*H*-pyrazol-5-ol scaffold and different aryl groups at position 4 of the 1*H*-pyrazol-5-ol nucleus.

2.3. In silico ADMET profile

In the present study, a computational study of the nine most active compounds was conducted to determine the surface area and other physicochemical properties according to the directions of Lipinski's rule (El-Helby et al., 2019). Lipinski suggested that the absorption capacity of a compound is much better if the molecule achieves at least three out of four of the following rules: (i) HB donor groups $\leq$ 5; (ii) HB acceptor groups $\leq$ 10; (iii) M. Wt < 500; (iv) logP < 5. In this study, compounds **3d**, **3m**, **4a-4b**, **4d**, **4g**, **4h-4i**, and **4l** follow all Lipinski's rules. All the highest active derivatives have a number of hydrogen bonding acceptor groups ranging between 3 and 6 and hydrogen bonding donors ranging between 1 and 3. Also, molecular weights are < 500 and log P < 5 and all these values agree with Lipinski's rules.

After assessing ADMET profiles of active compounds (Table 4), we can suggest that these derivatives have the advantage of better intestinal absorption in humans than Cipro and Flu, as all compounds showed Caco-2 and MDCK permeability higher than the control drugs. This preference may

Table 3 Antimicrobial activity data of synthesized compounds **2a-2p**, **3a-3x**, **4a-4p**, and **5a-5h.**

Entry	Code	Antibacterial					Antifungal	
		EC	PA	SF	MSSA	MRSA	CA	AN
1	**2a-2p**	–	–	–	–	–	–	–
2	**3a**	–	–	–	–	–	–	–
3	**3b**	–	–	–	64	128	–	–
4	**3c**	–	–	–	–	–	–	–
5	**3d**	–	–	–	**16**	**16**	–	–
6	**3e**	–	–	–	64	128	–	–
7	**3f-3k**	–	–	–	–	–	–	–
8	**3l**	–	–	–	64	64	–	–
9	**3m**	–	–	–	**4**	**8**	–	–
10	**3n-3o**	–	–	–	–	–	–	–
11	**3p**	–	–	–	128	128	–	–
12	**3q-3r**	–	–	–	–	–	–	–
13	**3s**	–	–	–	128	128	–	–
14	**3t**	–	–	–	128	256	–	–
15	**3u**	–	–	–	128	256	–	–
16	**3v**	–	–	–	32	32	–	–
17	**3w-3x**	–	–	–	–	–	–	–
18	**4a**	**16**	**–**	**16**	**4**	**8**	**16**	**16**
19	**4b**	–	–	–	**16**	**16**	–	–
20	**4c**	32	–	64	32	64	64	64
21	**4d**	–	–	–	**16**	**16**	–	–
22	**4e**	64	–	64	**16**	64	64	64
23	**4f**	64	–	64	64	64	64	64
24	**4g**	–	–	–	**16**	**16**	–	–
25	**4h**	32	–	32	32	64	32	**32**
26	**4i**	32	–	32	32	64	32	**32**
27	**4j**	64	–	64	64	64	64	64
28	**4k**	64	–	64	64	64	64	64
29	**4l**	32	–	32	32	64	32	**32**
30	**4m**	32	–	32	32	64	32	64
31	**4n**	64	–	64	64	64	64	64
32	**4o**	64	–	64	64	64	64	64
33	**4p**	**16**	–	64	32	64	64	64
34	**5a**	64	–	64	64	128	64	128
35	**5b**	64	–	64	64	128	64	128
36	**5c**	64	–	64	64	128	64	128
37	**5d**	64	–	64	64	128	64	128
38	**5e**	64	–	64	64	128	64	128
39	**5f**	64	–	64	64	64	64	64
40	**5g**	64	–	64	64	128	64	128
41	**5h**	64	–	64	64	64	64	64
42	**DMSO**	–	–	–	–	–	–	–
43	**Cipro**	**16**	**16**	**8**	**8**	**16**	NT	NT
44	**Flu**	NT	NT	NT	NT	NT	**16**	**128**

- : MIC > 1024 μg/mL, NT **-** not tested. **EC -** Escherichia coli ATCC 25922, **PA -** Pseudomonas aeruginosa ATCC 27853, **SF -** Streptococcus faecalis ATCC 29212, **MSSA -** Methicillin-susceptible strains of Staphylococcus aureus ATCC 29213, **MRSA -** Methicillin-resistant strains of Staphylococcus aureus ATCC 43300, **CA** - Candida albicans ATCC 10321, **AN** - Aspergillus niger ATCC 16404. **DMSO** - Dimethyl sulfoxide, **Cipro** - Ciprofloxacin, **Flu** - Fluconazole**. MIC** (μg/mL) ± 0.5 μg/mL. The values in bold (3d, 3m, 4a-4b, 4d-4e, 4g, 4h-4i, 4l, and 4p) highlight the best compounds with the best MIC values compared to positive controls (Ciprofloxacin, Fluconazole).

attribute to the superior lipophilic of the designed ligands, which would facilitate passage along different biological membranes (Beig et al., 2013). Accordingly, they may have remarkably good bioavailability after oral administration. In addition, all compounds showed good plasma protein binding capacity with PPB > 97% as compared to Cipro (PPB = 37%) and Flu (PPB = 62%). Studying the BBB (Blood-Brain Barrier) permeability, compounds **3d**, **3m**, **4a**, and **4d** demonstrated the best ability to penetrate the BBB, while Cipro is unable to penetrate.

The less skin permeant is the molecule, the more negative the log Kp (with Kp in cm/s). Therefore, all active compounds (log Kp in range of −6.23 to −4.86) showed better skin permeation than Cipro (log Kp at −9.09) and Flu (log Kp −7.92). The cytochrome enzymes could be weak to strong inhibit under the effect of active compounds especially CYP2C19,

Table 4 ADMET profile of the most active compounds, ciprofloxacin, and fluconazole.

Parameter	3d	3m	4a	4b	4d	4g	4h	4i	4l	Cipro	Flu
Absorption											
Caco-2 permeability	−4.835	−4.924	−4.850	−4.830	−4.881	−4.830	−4.884	−4.879	−4.881	−5.269	−4.950
MDCK permeability	4.4×10^{-5}	3.6×10^{-5}	9.4×10^{-5}	6.5×10^{-5}	4.6×10^{-5}	10.2×10^{-5}	5.9×10^{-5}	4.0×10^{-5}	5.2×10^{-5}	3.0×10^{-6}	2.8×10^{-5}
Pgp-inhibitor	− − −	− − −	− − −	–	+ +	–	− − −	− − −	–	− − −	− − −
Pgp-substrate	− − −	− − −	− − −	− − −	− − −	− − −	− − −	− − −	− − −	+ + +	− − −
HIA	+ + +	+ + +	+ + +	+ + +	+ + +	+ + +	+ + +	+ + +	+ + +	+ + +	+ + +
$F_{20\%}$	+ + +	+ + +	+ + +	+ + +	+ + +	+ + +	+ + +	+ + +	+ + +	+ + +	+ + +
$F_{30\%}$	+ + +	+ + +	+ + +	+ + +	+ + +	+ + +	+ + +	+ + +	+ + +	+ + +	+ + +
Distribution											
PPB (%)	100.312	98.077	99.657	99.781	100.619	98.208	98.077	97.295	98.312	37.456	61.763
VD (L/kg)	1.401	0.614	0.610	0.533	0.793	0.428	0.222	0.266	0.456	2.324	0.835
BBB penetration	+ +	+ +	+ +	+	+ +	+	+	+	+	− − −	+ + +
Fu (%)	0.869	1.644	0.866	0.834	0.760	1.217	1.545	2.083	1.303	78.856	51.002
Log Kp (cm/s)	−5.410	−6.230	−5.100	−5.100	−4.860	−5.370	−5.680	−5.690	−5.540	−9.090	−7.920
Metabolism											
CYP1A2 inhibitor	+ + +	+ + +	+ +	+ +	+ +	+ +	+ +	+ +	+ +	–	–
CYP1A2 substrate	–	− − −	+	+	+	–	–	–	+ +	–	–
CYP2C19 inhibitor	+ +	+ +	+ + +	+ + +	+ + +	+ + +	+ + +	+ + +	+ + +	− − −	+
CYP2C19 substrate	− − −	− − −	–	–	–	–	− − −	− − −	–	–	− − −
CYP2C9 inhibitor	+ +	+ +	+ + +	+ + +	+ + +	+ + +	+ + +	+ + +	+ + +	− − −	–
CYP2C9 substrate	+	+ +	+ + +	+ + +	+ + +	+ + +	+ + +	+ + +	+ + +	− − −	+
CYP2D6 inhibitor	+	+	+	+ +	+	+	+ +	+ +	+	− − −	–
CYP2D6 substrate	–	–	+ +	+ +	+ +	+ +	+ +	+ +	+ +	–	–
CYP3A4 inhibitor	+	+ +	+ + +	+ + +	+ + +	+ +	+ +	+ +	+ + +	− − −	–
CYP3A4 substrate	+	–	+ +	+ +	+ +	+ +	+	+	+ +	–	–
Excretion											
CL (mL/min/kg)	1.300	2.654	2.768	2.714	2.652	2.602	3.930	4.361	4.455	3.214	5.960
$T_{1/2}$	0.063	0.406	0.246	0.220	0.170	0.192	0.647	0.685	0.416	0.056	0.228
Toxicity											
hERG blockers	–	− − −	− − −	–	–	–	− − −	− − −	–	–	− − −
H-HT	–	–	–	–	–	+	+	+	+	+ + +	+ + +
DILI	+ + +	+ + +	+ + +	+ + +	+ + +	+ + +	+ + +	+ + +	+ + +	+ + +	+ + +
AMES toxicity	+ + +	+ + +	+ +	+ +	+ +	+ + +	+	+ +	+ +	–	+ +
Rat oral acute toxicity	− − −	− − −	− − −	− − −	–	–	–	–	− − −	–	+ + +
FDAMDD	+	+	–	–	+	–	− − −	–	–	+ +	+ +
Skin sensitization	+ +	+ + +	+	+	+	+	+	+ +	+ +	+	+ + +
Carcinogenicity	+ +	+ +	+	+	+	+ +	+ +	+ +	+ +	–	+ + +
Eye corrosion	− − −	− − −	− − −	− − −	− − −	− − −	− − −	− − −	− − −	− − −	− − −
Eye irritation	–	–	–	–	–	–	+ +	+	–	− − −	–
Respiratory toxicity	+ + +	+ + +	+ + +	+ + +	+ + +	+ + +	+ + +	+ + +	+ + +	+ +	+ +

Cipro: Ciprofloxacin, Flu: Fluconazole, Caco-2 permeability (optimal: higher than −5.15 Log unit). MDCK permeability (low permeability: $< 2 \times 10^{-6}$ cm/s, medium permeability:2–20 $\times 10^{-6}$ cm/s, high passive permeability: $> 20 \times 10^{-6}$ cm/s), Pgp: P-glycoprotein, HIA: Human Intestinal Absorption (−: < 30%, +: ≥ 30%), F: Bioavailability (−: < percent value, +: ≥ percent value), PPB: Plasma Protein Binding (optimal: < 90%), VD: Volume Distribution (optimal: 0.04–20 l/kg), BBB: Blood-Brain Barrier, Fu: The fraction unbound in plasms (low: < 5%, middle: 5 ∼ 20%, high: > 20%), Log Kp (skin permeation), CL: Clearance (low: < 5 mL/min/kg, moderate: 5–15 mL/min/kg, high: > 15 mL/min/kg), $T_{1/2}$ (category 1: long half-life (> 3h), category 0: short half-life (< 3h)), H-HT: Human Hepatotoxicity, DILI: Drug-Induced Liver Injury, FDAMDD: Maximum Recommended Daily Dose. The output value is the probability of being inhibitor/substrate/active/positive/high-toxicity/sensitizer/carcinogens/corrosives/irritants (category 1) or non-inhibitor/non-substrate/inactive/negative/low-toxicity/non-sensitizer/non-carcinogens/noncorrosives/nonirritants (category 0). For the classification endpoints, the prediction probability values are transformed into six symbols: 0–0.1(− − −), 0.1–0.3(− −), 0.3–0.5(−), 0.5–0.7 (+), 0.7–0.9(+ +), and 0.9–1.0(+ + +).

Table 5 In silico molecular docking results of active compounds and standard drugs.

Com pound	DHFR-B		GyrB		SrtA		TMK		Sap		DHFR-F		NMT	
	a	b	a	b	a	b	a	b	a	b	a	b	a	b
3d	−9.5	**1** ASN18	−8.4	**2** ARG44, ARG144	−7.8	**1** GLN120	−8.0	**2** ARG70						
3m	−9.7	**3** ASN18, ASP27, ILE14	−8.4	**1** ARG144	−8.0	**2** ARG139, GLN120	−8.0	**6** ASP91, GLY14, LYS15, SER13, THR16						
4a	−9.7	**4** ARG44, GLY94, LYS45, THR121	−7.4	**2** ASN54, SER128	−7.3	**0**	−7.6	**0**	−7.4	**1** THR222	−8.7	**0**	−9.4	**0**
4b	−9.6	**3** ARG44, GLY94, LYS45	−7.7	**0**	−7.5	**0**	−8.4	**3** ARG105, GLN101						
4d	−9.9	**4** GLY94, THR46, THR96	−8.3	**3** ARG84, ARG144, GLY85	−7.8	**0**	−8.6	**2** ARG105, GLN101						
4g	−9.7	**4** GLY94, THR46, THR96, THR121	−7.9	**3** ARG144, GLY85, SER128	−7.7	**0**	−8.5	**4** ARG105, GLN101, SER69						
4h									−7.5	**1** THR222	−8.6	**1** THR147	−9.4	**2** ASN392
4i									−7.7	**1** THR222	−8.6	**2** ALA11, GLU32	−9.3	**1** HIS227
4l									−7.6	**1** THR222	−8.4	**1** GLU32	−9.4	**1** HIS227
Cipro	−9.1	**1** SER49	−7.3	**1** ASP81	−6.8	**1** LYS117	−7.9	**3** ARG70, GLN101						
Flu									−6.4	**1** GLY85	−7.1	**5** ALA115, ARG56, ARG79, GLU116, LEU77	−7.9	**1** TYR225

The bacterial targets consist of DHFR-B: Dihydrofolate Reductase – Bacteria, GyrB: Gyrase B, SrtA: Sortase A, TMK: Thymidylate Kinase. The fungal targets consist of Sap: Secreted aspartic protease, DHFR-F: Dihydrofolate Reductase – Fungi, NMT: N-myristoyl Transferase. Cipro: Ciprofloxacin, Flu: Fluconazole. a: Affinity (Kcal/mol), b: Hydrogen bond (**number**, position).

CYP2C19, and CYP3A4 while Cipro and Flu couldn't. The strongest inhibition of CYP3A4, the main enzyme involved in drug metabolism exhibited on compounds **4a**, **4b**, **4d**, and **4l**.

The CL (clearance) is a significant parameter in deciding dose intervals as a tool for the assessment of excretion. Flu (CL = 5.69 mL/min/kg) exhibited the highest CL value compared to other ligands and was classified as a moderate clearance level ranging between 5 and 15 mL/min/kg. In contrast, all active compounds and Cipro showed lower CL values and were classified as low clearance levels (CL < 5 mL/min/kg). Thus, Flu could be excreted quicker and accordingly require shorter dosing intervals. Dissimilar to Flu, the new compounds exhibited slower clearance rates, which means the preference of possible extended dosing intervals of the novel derivatives.

Toxicity is the last parameter examined in the ADMET profile. As displayed in Table 4, all the new ligands, Cipro and Flu showed DILI (drug-induced liver injury and respiratory toxicity and did not exhibit hERG blockers and eye corrosion. The AMES toxicity and carcinogenicity of the new compounds and Flu are more than Cipro. On the other hand, compounds **3d**, **3m**, **4i**, **4l**, and Flu showed higher skin sensitization than other ligands and Cipro. In particular, all the new ligands showed lower H-HT (human hepatotoxicity) and FDAMDD (maximum recommended daily dose) than the reference drug.

2.4. In silico molecular docking studies

After ADMET profiling, docking studies were carried out to predict the most suitable binding pose and inhibition mechanism of newly synthesized derivatives. Based on the principle that similar compounds tend to bind to the same proteins, we predicted several reported protein targets against reference compounds (ciprofloxacin and fluconazole) and docked our active compounds against them. Seven different target proteins were selected including dihydrofolate reductase (DHFR-B), secreted aspartic protease (Sap), and *N*-myristoyl transferase (NMT) from *Candida albicans* as fungal target together with dihydrofolate reductase (DHFR-F), gyrase B (GyrB), thymidylate kinase (TMK), and sortase A (SrtA) from *Staphylococcus aureus* as bacterial target (Barakat et al., 2018). Among all these seven proteins, two proteins i.e. one protein (DHFR-B, dihydrofolate reductase - bacteria) from *S. aureus* and one protein (NMT, *N*-myristoyl transferase) from *C. albicans* presented good binding affinity with a higher affinity than −9.3 Kcal/mol, while all other targets showed weaker interactions with affinity in range of −7.3 to −8.7 Kcal/mol with active derivatives (Table 5).

The protein–ligand complex is formed through the electrostatic interactions of the binding interface include hydrogen bonds (both from side chains and backbones), salt bridges, and π-π stacking. Hydrogen bonding provides stability to protein molecules and selected protein–ligand interactions, thus being one of the most important for biological macromolecule interactions. Here in our study, compound **4d** being the most potent antibacterial agent against DHFR-B from *S. aureus* displayed the highest negative affinity of −9.9 Kcal/mol which is comparable to the standard drug ciprofloxacin (Cipro) with the affinity of −9.1 Kcal/mol. In addition, this compound established four hydrogen bonds with GLY94, THR46, and THR96 amino acids with bond length ranging between 2.16 and 2.99 Å while Cipro established only one hydrogen bond with SER49 (2.20 Å) and hence is considered as the best dock conformation in bacterial targets. Similarly, compounds **4a**,

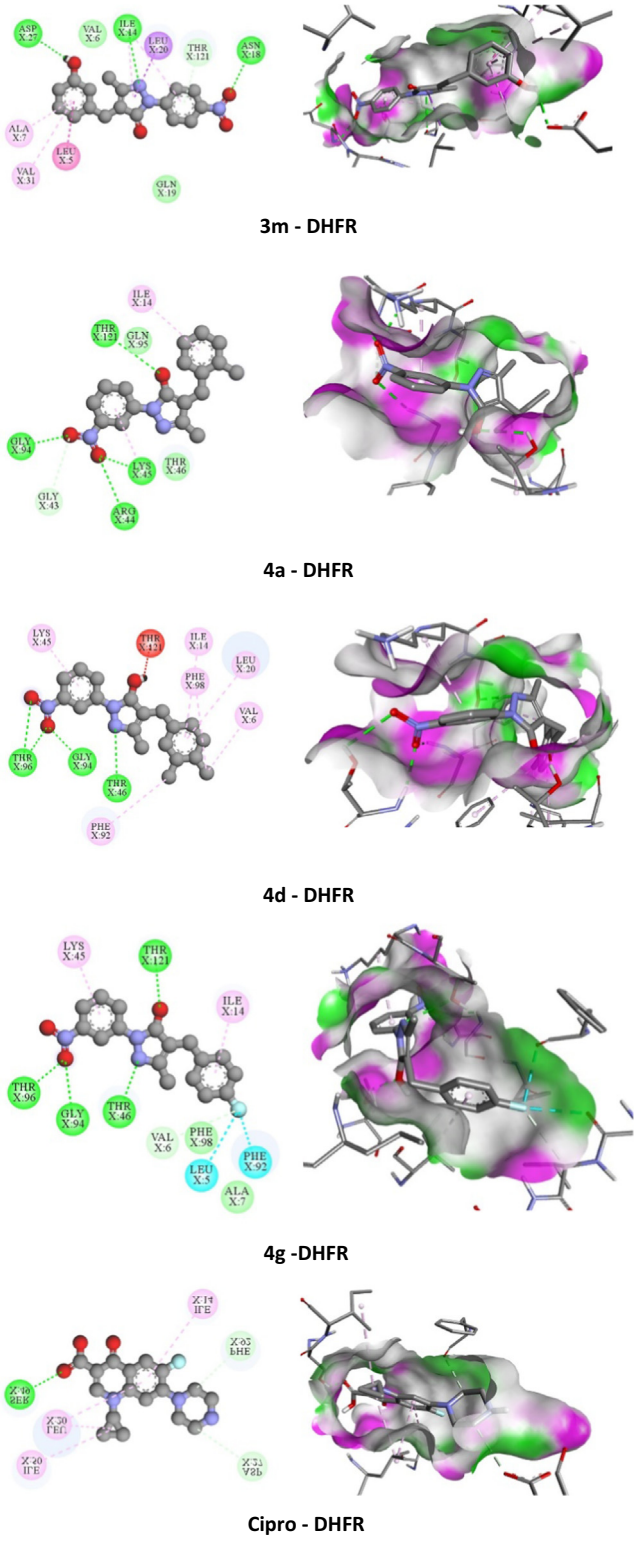

Fig. 3 2D and 3D representation of the interaction of the synthesized molecules 3 m, 4a, 4d, and 4 g and standard ciprofloxacin (Cipro) with dihydrofolate reductase (*S. aureus*).

4h, and **4l** being the most potent antifungal agents displayed a good affinity of −9.4 Kcal/mol which is comparable to the standard drug fluconazole (Flu) with the affinity of −7.9 Kcal/mol and molecular interactions with the NMT enzyme from *C. albicans*.

The compound **3m** established three hydrogen bonds (2.47–3.20 Å) with the affinity (−9.7 Kcal/mol) on DHFR-B receptor similar to compounds **4a**, and **4g** when compared with the standard drug Cipro (−9.1 Kcal/mol) (Fig. 3**)**. In addition, this compound established the most hydrogen bonds with six hydrogen bonds (2.32–3.00 Å) with ASP91, GLY14, LYS15, SER13, and THR16 amino acids with the affinity (−8.0 Kcal/mol) on TMK receptor. Similarly, compound **4g** also demonstrated a good affinity and ability to form hydrogen bonds on the DHFR-B and TMK receptors. These results suggested that DHFR-B and TMK (*S. aureus*) are the most likely targets for the antibacterial activity of these newly synthesized agents.

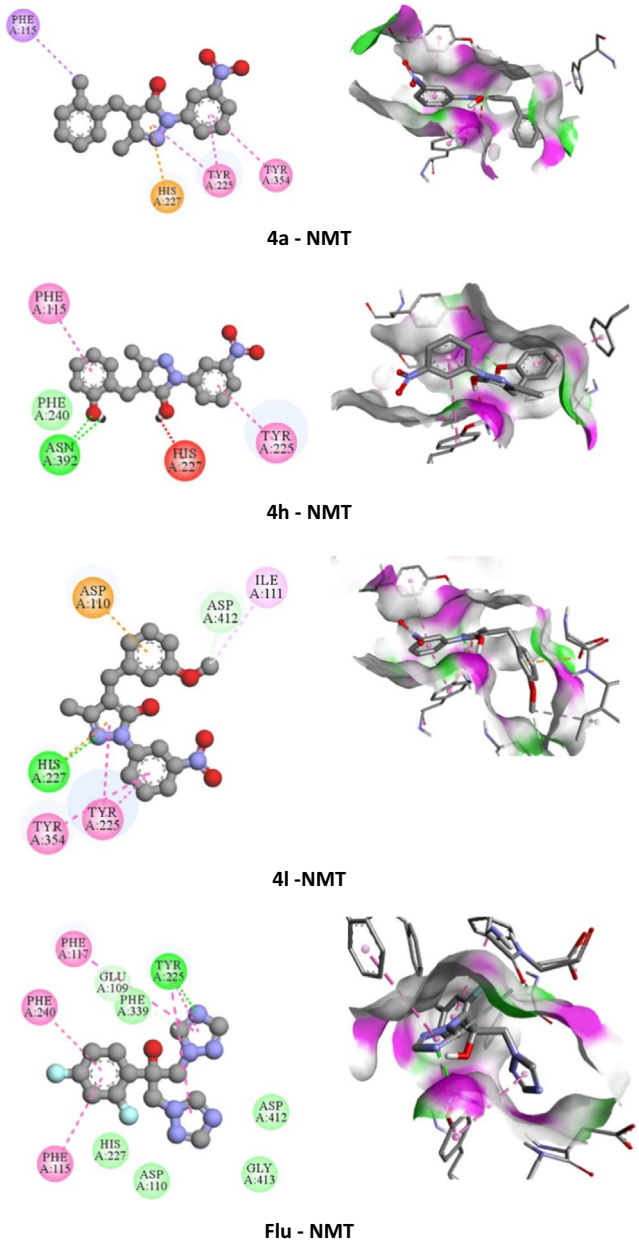

Fig. 4 2D and 3D representation of the interaction of the synthesized molecules 4a, 4 h, and 4 l and standard fluconazole (Flu) with *N*-myristoyl transferase (*C. albicans*).

On the crucial residues NMT, compound **4h** showed a number of significant electrostatic and hydrophobic interactions. Fig. 4 showed that the 2-hydroxy moiety attached to the benzene ring presented visible two hydrogen bonds with ASN392 at a distance of 2.45 and 2.97 Å. Apart from it, two hydrophobic interactions (π-π) were observed among benzene rings and two amino acids PHE115 and TYR225. Although compound **4l** has the same affinity for **4h**, compound **4l** has only established one hydrogen bond with HIS227 amino acid with a bond length of 2.70 A. These results predicted NMT (*C. albicans*) as the most probable target for the antifungal activity of these newly synthesized agents.

Among all the derivatives, compound **4a** showed the electrostatic and hydrophobic interactions with the crucial residue of the DHFR-B protein from *S. aureus* that resembles the co-crystallization ligand. As illustrated in Fig. 3, the substituted part of compound **4a** moved inside the cavity where both 3-nitro (3-NO_2) group in benzene ring at position 1 and hydroxy (—OH) group at position 5 of pyrazole nucleus were engaged in the formation of four halogen bonds with ARG44, GLY94, LYS45, and THR121 amino acids at 2.81, 2.77, 2.13 and 2.91 Å, respectively. Moreover, the nitro group displayed one carbon-hydrogen bond with the crucial residue GLY43 of the target protein with a bond length of 3.34 Å. Apart from it, benzene rings of **4a** were observed to establish hydrophobic interactions (π-alkyl) with ILE14 and LYS45 of DHFR-B protein. On the other hand, compound **4a** showed the highest negative affinity and established electrostatic interaction (π-cation) with HIS227 with a bond length of 4.27 Å and hydrophobic interactions (π-π) with PHE115, TYR225, and TYR354 of NMT protein from *C. albicans* (Fig. 4). The resulting docking may therefore be responsible for its potent antibacterial and antifungal activities.

3. Conclusion

In summary, sixty-four 1,4-disubstituted 3-methylpyrazol-5(4*H*)-one and 3-methyl-1*H*-pyrazol-5-ol derivatives including forty-five new compounds have been designed, synthesized, and evaluated for their antimicrobial activity. The antimicrobial activities were examined against Gram-positive bacteria, Gram-negative bacteria, and fungi. The values of the MIC against microorganisms showed that some compounds have significant inhibitory effects, especially compounds **3d**, **3m**, **4a**, **4d**, **4b**, and **4g** are potent for antibacterial activity while compounds **4a**, **4h**, **4i**, and **4l** is potent for antifungal activity. The compound **3m** showed significant and better activities against MSSA and MRSA than ciprofloxacin with MIC 4 and 8 μg/mL, respectively. In particular, compound **4a** exhibited the strongest activity among the synthesized compounds in both bacterial and fungal strains with MIC ranging between 4 and 16 μg/mL as compared to ciprofloxacin and fluconazole. From the structure–activity relationship (SAR), the presence of the chloro/ fluoro group in the aromatic ring at position 4 of 1-(3-nitrophenyl)pyrazolol scaffold is more desirable for enhanced antibacterial activity in **4a**, **4b**, **4d** and **4g**, and antifungal activity in **4a**. Molecular docking predicted that DHFR (dihydrofolate reductase) protein from *S. aureus* and NMT (*N*-myristoyl transferase) protein from *C. albicans* are the most suitable targets for the antimicrobial activities. Compounds **4a** being the most potent antifungal agents

displayed a good affinity of −9.4 Kcal/mol with the NMT enzyme from *C. albicans* and showed a good affinity of −9.7 Kcal/mol with the crucial residue of the DHFR-B protein from *S. aureus* that resembles the co-crystallization ligand. On the other hand, compound **3m** established three hydrogen bonds with the affinity (−9.7 Kcal/mol) with DHFR-B receptor similar to compound **4a**. ADMET profile was evaluated for the nine most active compounds in comparison to ciprofloxacin and fluconazole as reference drugs. The obtained results suggest that our derivatives showed a good ADMET profile. All compounds show physical–chemical properties of fragment and lead-like compounds which are of great interest for further drug development. This work paved the way for the synthesis of more potent compounds based on 1-(3-nitrophenyl)pyrazolol scaffolds and explore their various and potential biological activities as well as their mechanism of action.

4. Experimental section

4.1. Materials

All the reactions were carried out under an inert atmosphere of nitrogen. TLC was performed on pre-coated aluminum sheets of silica (60 F_{254} nm) and visualized by shortwave UV light at λ 254. Column chromatography uses 0.040–0.063 mm granular silica gel (Merck).

Melting points were determined on a Sanyo-Gallenkamp melting point apparatus. UV–Vis absorption spectra were recorded on a Perkin Elmer Lambda 40p spectrometer. IR spectra were recorded on an IRAffinity-1S. NMR spectra were recorded on a Bruker Avance 500 NMR Spectrometer ((^{1}H NMR 500 MHz, ^{13}C NMR 125 MHz). Chemical shifts were measured in δ (ppm). Mass spectrometry was measured on 1100 series LC-MS Trap Agilent.

4.2. Experimental procedures

*4.2.1. General procedure for the synthesis of 1-aryl-3-methylpyrazol-5(4H)-one (**1a-1b**)*

A mixture of 3-nitrophenylhydrazine or 4-nitrophenylhydrazine hydrochloride (0.03 mol) and ethyl acetoacetate (0.03 mol) was taken in absolute alcohol (90 mL) and refluxed for 2 h. After completion of the reaction, the excess solvent was distilled off and the resultant residue was poured on crushed ice to obtain the yellow long needle-shaped crystals. The precipitated solids were collected by filtration and recrystallized using ethanol.

*3-Methyl-1-(3-nitrophenyl)pyrazol-5(4H)-one **(1a):*** yellow solid, yield 52%, mp 185–187 °C. IR (ν, cm^{-1}): 3194.1 (C—H), 1624.1 (C═O), 1525.7 and 1346.3 (NO_2). ^{1}H NMR (500 MHz, DMSO d_6, δ ppm): 12.04 (1H, s, —OH), 8.60 (1H, s, H_{Ar}), 8.20 (1H, d, J = 8.0 Hz, H_{Ar}), 8.03 (1H, dd, J = 8.5, 1.5 Hz, H_{Ar}), 7.20 (1H, t, J = 8.0 Hz, H_{Ar}), 5.43 (1H, s, —CH═), 2.15 (3H, s, —CH_3). ^{13}C NMR (125 MHz, DMSO d_6, δ ppm): 159.8, 148.1, 139.6, 130.6, 130.5, 125.2, 123.3, 119.0, 118.6, 113.5, 111.6, 43.2, 16.7, 14.0. LC-MS (m/z) $[M+H]^+$ calcd for $C_{10}H_{10}N_3O_3$ 220.0717, found 220.0737.

*3-Methyl-1-(4-nitrophenyl)pyrazol-5(4H)-one **(1b):*** yellow solid, yield 60%, mp 221–223 °C. IR (ν, cm^{-1}): 3122.5 and 2960.8 (C—H), 1727.7 (C═O) and 1628.5 (C═N). ^{1}H NMR (500 MHz, DMSO d_6, δ ppm): 12.20 (1H, s, —OH), 8.29 (2H, d, J = 9.0 Hz, H_{Ar}), 8.04 (2H, d, J = 9.0 Hz, H_{Ar}), 1H, 5.42 (s, —CH═), 2.14 (3H, s, —CH_3). LC-MS (m/z) $[M+H]^+$ calcd for $C_{10}H_{10}N_3O_3$ 220.0717, found 220.0722.

*4.2.2. General procedure for the synthesis of 4-arylidene-1-aryl-3-methylpyrazol-5(4H)-one (**2a-2p**, **3a-3x**)*

An equimolar mixture of substituted aromatic aldehydes (0.10 mol) and 1-aryl-3-methylpyrazol-5(4*H*)-one (0.10 mol) in acetic acid (20 mL) and sodium acetate (0.01 mol) was refluxed for 3 h at 80 °C. After completion, the reaction mixture was allowed to cool, filtered, and poured on crushed ice. The precipitated solids were collected by filtration and recrystallized using acetic acid.

*4.2.3. Microwave assisted synthesis 4-arylidene-1-aryl-3-methylpyrazol-5(4H)-one (**2a-2p**, **3a-3x**)*

An equimolar mixture of substituted aromatic aldehydes (0.01 mol) and 1-aryl-3-methylpyrazol-5(4*H*)-one (0.01 mol) in acetic acid (2 mL) and sodium acetate (0.001 mol) were placed in a microwave (MW) oven and irradiated at a power of 300 W for 10 min. After completion, the reaction mixture was allowed to cool, filtered, and poured on crushed ice. The solid thus separated was collected by filtration and recrystallized from acetic acid.

*4-(2-Chlorobenzylidene)-3-methyl-1-(3-nitrophenyl)pyrazol-5(4H)-one **(2a)***: yellow solid, yield 77%, mp 241–243 °C. IR (ν, cm^{-1}): 3085.8 (C—H), 1685.8 (C═O), 1614.4 (C═C), 1521.8 and 1346.3 (NO_2). ^{1}H NMR (500 MHz, DMSO d_6, δ ppm): 8.75–8.73 (2H, m, H_{Ar}), 8.54 (1H, dd, J = 8.0, 1.5 Hz, H_{Ar}), 8.34 (1H, ddd, J = 8.5, 2.0, 1.5 Hz, H_{Ar}), 8.30 (1H, ddd, J = 8.5, 2.5, 1.0 Hz, H_{Ar}), 8.08 (1H, ddd, J = 8.5, 2.0, 1.0 Hz, H_{Ar}), 8.06–8.04 (2H, m, H_{Ar} and —CH═), 8.03 (1H, s, —CH═), 7.79–7.72 (3H, m, H_{Ar}), 7.68–7.65 (2H, m, H_{Ar}), 7.62–7.59 (2H, m, H_{Ar}), 7.53–7.48 (2H, m, H_{Ar}), 2.94 (3H, s, —CH_3), 2,07 (3H, s, —CH_3). ^{13}C NMR (125 MHz, DMSO d_6, δ ppm): 160.1, 159.7, 152.1, 148.8, 137.2, 136.2. 134.2, 133.1, 133.0, 132.7, 132.6, 131.2, 130.6, 130.6, 125.1, 125.1, 123.5, 123.2, 120.0, 120.0, 119.1, 119.0, 114.6, 114.4, 111.9, 111.6, 14.4, 12.8. LC-MS (m/z) $[M+H]^+$ calcd for $C_{17}H_{13}ClN_3O_3$ 342.0640, found 342.0635.

*4-(4-Chlorobenzylidene)-3-methyl-1-(3-nitrophenyl)pyrazol-5(4H)-one **(2b)***: yellow solid, yield 78%, mp 271–273 °C. IR (ν, cm^{-1}): 3130.5 (C—H), 1685.8 (C═O), 1612.5 (C═C), 1523.8 (NO_2). ^{1}H NMR (500 MHz, DMSO d_6, δ ppm): 8.83 (1H, t, J = 2.5 Hz, H_{Ar}), 8.61 (2H, d, J = 8.5 Hz, H_{Ar}), 8.35 (1H, d, J = 8.0 Hz, H_{Ar}), 8.05 (1H, dd, J = 8.0, 2.0 Hz, H_{Ar}), 7.93 (1H, s, —CH═), 7.75 (1H, t, J = 8.5 Hz, H_{Ar}), 7.68 (2H, d, J = 8.5 Hz, H_{Ar}), 2.30 (3H, s, —CH_3). ^{13}C NMR (125 MHz, DMSO d_6, δ ppm): 161.5, 152.4, 147.9, 147.1, 138.5, 137.7, 134.8, 131.2, 130.0, 128.3, 126.3, 123.3, 118.4, 111.8, 12.5. LC-MS (m/z) $[M+H]^+$ calcd for $C_{17}H_{13}ClN_3O_3$ 342.0640, found 342.0728.

*4-(2-Chloro-6-fluorobenzylidene)-3-methyl-1-(3-nitrophenyl)pyrazol-5(4H)-one **(2c)***: orange solid, yield 78%, mp 280–282 °C. IR (ν, cm^{-1}): 3099.6 (C—H), 1708.9 (C═O), 1614.4 (C═C), 1527.6 and 1342.5 (NO_2). ^{1}H NMR (500 MHz, DMSO d_6, δ ppm): 8.71 (1H, t, J = 2.0 Hz, H_{Ar}), 8.68 (1H, t, J = 2.0 Hz, H_{Ar}), 8.32 (1H, ddd, J = 8.5, 2.0, 1.0 Hz, H_{Ar}), 8.25 (1H, ddd, J = 8.5, 2.0, 1.0 Hz, H_{Ar}), 8.08 (1H, ddd, J = 8.5, 2.5, 1.0 Hz, H_{Ar}), 8.04 (1H, ddd, J = 8.5, 2.5, 1.0 Hz, H_{Ar}), 7.91 (1H, s, —CH═), 7.86 (1H, s, —CH═), 7.78 (1H, t, J = 8.5 Hz, H_{Ar}), 7.72 (1H, t, J = 8.5 Hz, H_{Ar}), 7.66–7.56 (3H, m, H_{Ar}), 7.49 (1H, d, J = 8.0 Hz, H_{Ar}), 7.46 (1H, d, J = 8.0 Hz, H_{Ar}), 7.37 (1H, t, J = 9.0 Hz, H_{Ar}), 2.42 (3H, s, —CH_3), 1.98 (3H, s, —CH_3).

^{13}C NMR (125 MHz, DMSO d_6, δ ppm): 160.6, 158.8, 151.3, 148.0, 138.4, 136.5, 135.6, 133.6, 133.2, 132.8, 132.7, 131.2, 130.7, 130.6, 126.0, 125.4, 123.5, 123.3, 120.1, 119.9, 119.2, 118.9, 114.7, 114.5, 111.9, 111.6, 14.4, 12.8. LC-MS (*m*/*z*) $[M+H]^+$ calcd for $C_{17}H_{12}ClFN_3O_3$ 360.0546, found 360.0621.

4-(3,4-Dichlorobenzylidene)-3-methyl-1-(3-nitrophenyl)pyrazol-5(4H)-one ***(2d)***: red solid, yield 81%, mp 273–275 °C. IR (ν, cm^{-1}): 3090.0 (C—H), 1681.9 (C═O), 1614.4 (C═C), 1525.7 and 1344.4 (NO_2). ^{1}H NMR (500 MHz, DMSO d_6, δ ppm): 8.96 (1H, d, J = 2.0 Hz, H_{Ar}), 8.77 (1H, t, J = 2.5 Hz, H_{Ar}), 8.46 (1H, d, J = 8.5, 2.0 Hz, H_{Ar}), 8.34 (1H, ddd, J = 8.5, 2.0, 1.0 Hz, H_{Ar}), 8.05 (1H, ddd, J = 8.5, 2.5, 1.0 Hz, H_{Ar}), 7.90 (1H, s, —CH═), 7.87 (1H, d, J = 8.5 Hz, H_{Ar}), 7.75 (1H, t, J = 8.0 Hz, H_{Ar}), 2.37 (3H, s, —CH_3). ^{13}C NMR (125 MHz, DMSO d_6, δ ppm): 161.4, 152.4, 147.9, 145.6, 138.4, 135.3, 134.1, 133.0, 132.7, 131.1, 130.5, 130.1, 127.4, 123.4, 118.6, 111.8, 12.6. LC-MS (*m*/*z*) $[M+H]^+$ calcd for $C_{17}H_{12}N_3O_3Cl_2$ 376.0250, found 376.0475.

4-(2,4-Dimethoxybenzylidene)-3-methyl-1-(3-nitrophenyl)pyrazol-5(4H)-one ***(2e)***: yellow solid, yield 69%, mp 251–252 °C. IR (ν, cm^{-1}): 3130.5 (C—H), 1697.4 (C═O), 1602.9 (C═C), 1521.8 (NO_2). ^{1}H NMR (500 MHz, DMSO d_6, δ ppm): 8.78 (1H, t, J = 2.0 Hz, H_{Ar}), 8.72 (1H, d, J = 1.5 Hz, H_{Ar}), 8.39 (1H, dd, J = 8.0, 1.5 Hz, H_{Ar}), 8.14 (1H, dd, J = 8.5, 2.0 Hz, H_{Ar}), 8.02 (1H, dd, J = 8.5, 1.5 Hz, H_{Ar}), 7.81 (1H, s, —CH═), 7.73 (1H, t, J = 8.5 Hz, H_{Ar}), 7.19 (1H, d, J = 8.0 Hz, H_{Ar}), 3.91(3H, s, —OCH_3), 3.81 (3H, s, —OCH_3), 2.36 (3H, s, —CH_3). ^{13}C NMR (125 MHz, DMSO d_6, δ ppm): 162.1, 154.0, 152.6, 149.2, 148.2, 147.9, 138.9, 130.5, 130.0, 126.0, 123.4, 122.8, 118.2, 116.5, 111.8, 111.4, 55.7, 55.5, 12.7. LC-MS (*m*/*z*) $[M+H]^+$ calcd for $C_{19}H_{18}N_3O_5$ 368.1241, found 368.0683.

4-(3,4-Dimethoxybenzylidene)-3-methyl-1-(3-nitrophenyl)pyrazol-5(4H)-one ***(2f)***: red solid, yield 75%, mp 237–239 °C. IR (ν, cm^{-1}): 2945.3 and 2841.1 (C—H), 1697.4 (C═O), 1602.8 (C═C), 1521.8 (NO_2). ^{1}H NMR (500 MHz, DMSO d_6, δ ppm): 9.34 (1H, d, J = 9.0 Hz, H_{Ar}), 8.84 (1H, s, H_{Ar}), 8.36 (1H, d, J = 8.0 Hz, H_{Ar}), 8.02 (1H, d, J = 9.0 Hz, H_{Ar}), 7.99 (1H, s, —CH═), 7.72 (1H, t, J = 8.5 Hz, H_{Ar}), 6.75 (1H, d, J = 9.0 Hz, H_{Ar}), 6.70 (1H, s, H_{Ar}), 3.96 (3H, s, —OCH_3), 3.92 (3H, s, —OCH_3), 2.32 (3H, s, —CH_3). ^{13}C NMR (125 MHz, DMSO d_6, δ ppm): 162.2, 154.0, 152.7, 149.3, 148.2, 148.0, 139.0, 130.5, 130.1, 126.0, 123.5, 122.8, 118.3, 116.6, 111.9, 111.5, 55.7, 55.6, 12.7. LC-MS (*m*/*z*) $[M+H]^+$ calcd for $C_{19}H_{18}N_3O_5$ 368.1241, found 368.1595.

4-(4-Fluorobenzylidene)-3-methyl-1-(3-nitrophenyl)pyrazol-5(4H)-one ***(2g)***: yellow solid, yield 86%, mp 278–280 °C. IR (ν, cm^{-1}): 3109.2 (C—H), 1691.6 (C═O), 1614.4 (C═C), 1508.3 and 1346.3 (NO_2). ^{1}H NMR (500 MHz, DMSO d_6, δ ppm): 8.83 (1H, t, J = 2.0 Hz, H_{Ar}), 8.72 (2H, dd, J = 9.0, 6.0 Hz, H_{Ar}), 8.35 (1H, dd, J = 8.5, 1.5 Hz, H_{Ar}), 8.05 (1H, dd, J = 8.0, 1.5 Hz, H_{Ar}), 7.94 (s, 1H, —CH═), 7.75 (1H, t, J = 8.5 Hz, H_{Ar}), 7.45 (2H, t, J = 9.0 Hz, H_{Ar}), 2.39 (s, 3H, —CH_3). ^{13}C NMR (125 MHz, DMSO d_6, δ ppm): 161.7, 152.6, 147.9, 147.6, 138.7, 136.5, 136.4, 130.1, 123.4, 118.5, 115.6, 115.5, 111.8, 12.7. LC-MS (*m*/*z*) $[M+H]^+$ calcd for $C_{17}H_{13}FN_3O_3$ 326.0935, found 326.0806.

4-(2-Hydroxybenzylidene)-3-methyl-1-(3-nitrophenyl)pyrazol-5(4H)-one ***(2h)***: yellow solid, yield 74%, mp 280–283 °C. IR (ν, cm^{-1}): 3302.1 (OH), 2916.4 and 2848.9 (C—H), 1730.2 (C═O), 1527.6 (NO_2). ^{1}H NMR (500 MHz, DMSO d_6, δ ppm): 9.31 (1H, s, —OH), 9.03 (1H, dd, J = 8.0, 1.5 Hz, H_{Ar}), 8.82 (1H, t, J = 2.5 Hz, H_{Ar}), 8.35 (1H, ddd, J = 8.5, 2.0, 1.0 Hz, H_{Ar}), 8.10 (1H, s, —CH═), 8.03 (1H, ddd, J = 8.5, 2.0, 1.0 Hz, H_{Ar}), 7.73 (1H, t, J = 8.5 Hz, H_{Ar}), 7.49 (1H, t, J = 8.5 Hz, H_{Ar}), 7.01 (1H, d, J = 7.5 Hz, H_{Ar}), 6.95 (1H, t, J = 8.0 Hz, H_{Ar}), 2.35 (3H, s, —CH_3). ^{13}C NMR (125 MHz, DMSO d_6, δ ppm): 162.6, 159.4, 158.1, 152.9, 148.0, 142.9, 139.0, 136.3, 132.9, 130.5, 124.0, 123.5, 123.2, 119.7, 118.9, 118.6, 115.9, 111.8, 111.6, 17.1, 13.0. LC-MS (*m*/*z*) $[M-H]^-$ calcd for $C_{17}H_{12}N_3O_4$ 322.0833, found 322.0767.

4-(4-Hydroxybenzylidene)-3-methyl-1-(3-nitrophenyl)pyrazol-5(4H)-one ***(2i)***: yellow solid, yield 75%, mp 298–300 °C. IR (ν, cm^{-1}): 3310.0 (OH), 3107.3 (C—H), 1662.8 (C═O), 1587.4 (C═C), 1514.1 and 1321.2 (NO_2). ^{1}H NMR (500 MHz, DMSO d_6, δ ppm): 9.10 (1H, s, —OH), 8.86 (1H, t, J = 2.5 Hz, H_{Ar}), 8.63 (2H, d, J = 9.0 Hz, H_{Ar}), 8.37 (1H, ddd, J = 8.5, 2.0, 1.0 Hz, H_{Ar}), 8.03 (1H, ddd, J = 8.0, 2.5, 1.0 Hz, H_{Ar}), 7.77 (1H, s, —CH═), 7.73 (1H, t, J = 8.5 Hz, H_{Ar}), 6.97 (2H, d, J = 9.0 Hz, H_{Ar}), 2.36 (3H, s, —CH_3). ^{13}C NMR (125 MHz, DMSO d_6, δ ppm): 163.5, 162.4, 153.1, 149.7, 148.0, 139.2, 137.7, 130.5, 124.8, 123.5, 121.8, 118.5, 116.0, 111.8, 13.2. LC-MS (*m*/*z*) $[M-H]^-$ calcd for $C_{17}H_{12}N_3O_4$ 322.0833, found 322.0800.

4-(3-Hydroxy-4-methoxybenzylidene)-3-methyl-1-(3-nitrophenyl)pyrazol-5(4H)-one ***(2j)***: orange solid, yield 63%, mp 212–214 °C. IR (ν, cm^{-1}): 3408.2 (OH), 3080.3 (C—H), 1668.4 (C═O), 1564.2 (C═C), 1529.6 and 1344.4 (NO_2). ^{1}H NMR (500 MHz, DMSO d_6, δ ppm): 9.50 (1H, s, —OH), 8.87 (1H, t, J = 2.0 Hz, H_{Ar}), 8.44 (1H, d, J = 2.0 Hz, H_{Ar}), 8.36 (1H, dd, J = 8.5, 2.0 Hz, H_{Ar}), 8.04–8.01 (2H, m, H_{Ar}), 7.73 (1H, s, —CH═), 7.73 (1H, t, J = 8.5 Hz, H_{Ar}), 7.15 (1H, d, J = 8.5 Hz, H_{Ar}), 3.91 (3H, s, —OCH_3), 2.36 (3H, s, —CH_3). ^{13}C NMR (125 MHz, DMSO d_6, δ ppm): 162.3, 153.4, 153.1, 149.9, 148.0, 146.2, 139.1, 130.4, 129.7, 126.3, 123.5, 122.6, 119.9, 118.5, 111.8, 111.6, 55.8, 13.1. LC-MS (*m*/*z*) $[M-H]^-$ calcd for $C_{18}H_{14}N_3O_5$ 352.0939, found 352.0936.

4-(4-Hydroxy-3-methoxybenzylidene)-3-methyl-1-(3-nitrophenyl)pyrazol-5(4H)-one ***(2k)***: orange solid, yield 59%, mp 220–222 °C. IR (ν, cm^{-1}): 3410.1 (OH), 3080.3 (C—H), 1668.4 (C═O), 1564.2 (C═C), 1527.6 and 1344.4 (NO_2). ^{1}H NMR (500 MHz, DMSO d_6, δ ppm): 10.62 (1H, s, —OH), 8.79 (1H, t, J = 2.5 Hz, H_{Ar}), 8.71 (1H, d, J = 2.0 Hz, H_{Ar}), 8.39 (1H, dd, J = 8.5, 1.5 Hz, H_{Ar}), 8.05 (1H, dd, J = 8.5, 2.0 Hz, H_{Ar}), 8.00 (1H, dd, J = 8.5, 2.0 Hz, H_{Ar}), 7.74 (1H, s, —CH═), 7.72 (1H, t, J = 8.5 Hz, H_{Ar}), 6.96 (1H, d, J = 8.5 Hz, H_{Ar}), 3.89 (3H, s, —OCH_3), 2.34 (3H, s, —CH_3). ^{13}C NMR (125 MHz, DMSO d_6, δ ppm): 162.5, 153.4, 153.0, 150.0, 148.0, 147.4, 139.2, 131.4, 130.4, 125.2, 123.6, 121.7, 118.5, 117.3, 115.7, 111.9, 55.7, 13.1. LC-MS (*m*/*z*) $[M-H]^-$ calcd for $C_{18}H_{14}N_3O_5$ 352.0939, found 352.0903.

4-(3-Methoxybenzylidene)-3-methyl-1-(3-nitrophenyl)pyrazol-5(4H)-one ***(2l)***: yellow solid, yield 77%, mp 184–188 °C. IR (ν, cm^{-1}): 3124.7 and 3093.8 (C—H), 1687.7 (C═O), 1579.7 (C═C), 1508.3 (NO_2). ^{1}H NMR (500 MHz, DMSO d_6, δ ppm): 8.78 (1H, t, J = 2.5 Hz, H_{Ar}), 8.39 (1H, t, J = 2.0 Hz, H_{Ar}), 8.37 (1H, ddd, J = 8.5, 2.0, 1.0 Hz, H_{Ar}), 8.07–8.03 (2H, m, H_{Ar}), 7.89 (1H, s, —CH═), 7.75 (1H, t, J = 8.0 Hz, H_{Ar}), 7.50 (1H, t, J = 8.0 Hz, H_{Ar}), 7.24 (1H, ddd, J = 8.5, 2.5, 1.0 Hz, H_{Ar}), 3.86 (3H, s, —OCH_3), 2.38 (3H, s, —CH_3). ^{13}C

NMR (125 MHz, DMSO d_6, δ ppm): 161.8, 159.0, 152.9, 149.3, 148.0, 138.8, 133.9, 130.4, 129.6, 126.8, 126.2, 123.6, 119.8, 118.7, 117.9, 111.9, 55.3, 13.1. LC-MS (*m*/*z*) $[M+H]^+$ calcd for $C_{18}H_{16}N_3O_4$ 338.1135, found 338.1110.

4-(4-Methoxybenzylidene)-3-methyl-1-(3-nitrophenyl)pyrazol-5(4H)-one ***(2m)***: yellow solid, yield 75%, mp 188–190 °C. IR (ν, cm^{-1}): 3124.7 and 3093.8 (C—H), 1687.7 (C=O), 1579.7 (C=C), 1508.3 (NO_2). ^1H NMR (500 MHz, DMSO d_6, δ ppm): 8.82 (1H, t, J = 2.0 Hz, H_{Ar}), 8.68 (2H, d, J = 9.0 Hz, H_{Ar}), 8.35 (1H, dd, J = 8.0, 1.5 Hz, H_{Ar}), 8.00 (1H, dd, J = 8.0, 1.5 Hz, H_{Ar}), 7.80 (1H, s, —CH=), 7.71 (1H, t, J = 8.5 Hz, H_{Ar}), 7.14 (2H, d, J = 9.0 Hz, H_{Ar}), 3.90 (3H, s, —OCH_3), 2.35 (3H, s, —CH_3). ^{13}C NMR (125 MHz, DMSO d_6, δ ppm): 163.9, 162.3, 153.0, 149.2, 147.3, 139.1, 137.0, 130.4, 126.0, 123.5, 123.0, 118.5, 114.4, 111.8, 55.7, 13.1. LC-MS (*m*/*z*) $[M+H]^+$ calcd for $C_{18}H_{16}N_3O_4$ 338.1135, found 338.1130.

3-Methyl-4-(4-(methylthio)benzylidene)-1-(3-nitrophenyl)pyrazol-5(4H)-one ***(2n)***: yellow solid, yield 74%, mp 200–202 °C. IR (ν, cm^{-1}): 2920.2 (C—H), 1678.1 (C=O), 1608.6 (C=C), 1523.8 and 1327.0 (NO_2). ^1H NMR (500 MHz, DMSO d_6, δ ppm): 8.84 (1H, t, J = 2.0 Hz, H_{Ar}), 8.59 (2H, d, J = 8.5 Hz, H_{Ar}), 8.34 (1H, ddd, J = 8.0, 2.0, 1.0 Hz, H_{Ar}), 8.04 (1H, ddd, J = 8.5, 2.0, 1.0 Hz, H_{Ar}), 7.84 (1H, s, —CH=), 7.74 (1H, t, J = 8.0 Hz, H_{Ar}), 7.45 (2H, d, J = 8.5 Hz, H_{Ar}), 2.56 (3H, s, -SCH_3), 2.38 (3H, s, —CH_3). ^{13}C NMR (125 MHz, DMSO d_6, δ ppm): 161.8, 152.5, 148.3, 147.9, 146.8, 138.8, 133.9, 130.0, 128.9, 124.6, 124.3, 123.3, 118.2, 111.7, 13.6, 12.6. LC-MS (*m*/*z*) $[M-H]^-$ calcd for $C_{18}H_{14}N_3O_3S$ 352.0761, found 352.0681.

3-Methyl-4-(3-nitrobenzylidene)-1-(3-nitrophenyl)pyrazol-5(4H)-one ***(2o)***: red solid, yield 85%, mp 264–266 °C. IR (ν, cm^{-1}): 3072.6 (C—H), 1691.7 (C=O), 1616.3 (C=C), 1516.0 (NO_2). ^1H NMR (500 MHz, DMSO d_6, δ ppm): 9.51 (1H, t, J = 2.0 Hz, H_{Ar}), 8.84 (1H, d, J = 8.0 Hz, H_{Ar}), 8.74 (1H, t, J = 2.0 Hz, H_{Ar}), 8.43 (1H, dd, J = 8.0, 1.5 Hz, H_{Ar}), 8.33 (1H, dd, J = 8.5, 1.0 Hz, H_{Ar}), 8.07 (1H, s, —CH=), 8.05 (1H, ddd, J = 8.0, 1.5, 1.0 Hz, H_{Ar}), 7.86 (1H, t, J = 8.0 Hz, H_{Ar}), 7.74 (1H, t, J = 8.5 Hz, H_{Ar}), 2.36 (3H, s, —CH_3). ^{13}C NMR (125 MHz, DMSO d_6, δ ppm): 161.6, 152.8, 148.0, 147.8, 146.3, 138.6, 134.8, 130.1, 129.7, 128.5, 127.0, 125.4, 124.0, 123.7, 119.6, 112.0, 13.0. LC-MS (*m*/*z*) $[M+H]^+$ calcd for $C_{17}H_{13}N_4O_5$ 353.0880, found 353.0886.

4-(Benzo[d][1,3]dioxol-5-ylmethylene)-3-methyl-1-(3-nitrophenyl)pyrazol-5(4H)-one ***(2p)***: yellow solid, yield 80%, mp 215–217 °C. IR (ν, cm^{-1}): 2918.3 (C—H), 1689.6 (C=O), 1523.8 and 1344.4 (NO_2). ^1H NMR (500 MHz, DMSO d_6, δ ppm): 8.81 (1H, t, J = 2.0 Hz, H_{Ar}), 8.66 (1H, d, J = 1.5 Hz, H_{Ar}), 8.38 (1H, dd, J = 8.5, 1.5 Hz, H_{Ar}), 8.04–8.02 (2H, m, H_{Ar}), 7.80 (1H, s, —CH=), 7.73 (1H, t, J = 8.5 Hz, H_{Ar}), 7.17 (1H, d, J = 8.0 Hz, H_{Ar}), 6.22 (2H, s, —OCH_2O-), 2.36 (3H, s, —CH_3). ^{13}C NMR (125 MHz, DMSO d_6, δ ppm): 162.2, 153.0, 152.5, 149.4, 148.0, 147.7, 139.0, 133.2, 130.5, 127.7, 123.6, 123.3, 118.7, 111.9, 108.7, 102.5, 13.1. LC-MS (*m*/*z*) $[M+H]^+$ calcd for $C_{18}H_{14}N_3O_5$ 352.0928, found 352.0852.

4-(2-Chlorobenzylidene)-3-methyl-1-(4-nitrophenyl)pyrazol-5(4H)-one ***(3a)***: orange solid, yield 81%, mp 227–229 °C. IR (ν, cm^{-1}): 3124.7 (C—H), 1685.0 (C=O), 1614.4 (C=N), 1521.8 (C=C). ^1H NMR (500 MHz, DMSO d_6, δ ppm): 8.52 (1H, dd, J = 8.0, 1.5 Hz, H_{Ar}), 8.34 (2H, d, J = 9.5 Hz, H_{Ar}), 8.30 (2H, d, J = 9.0 Hz, H_{Ar}), 8.18 (2H, d, J = 9.5 Hz, H_{Ar}), 8.15 (2H, d, J = 9.5 Hz, H_{Ar}), 8.06 (1H, s, —CH=), 8.00 (1H, s, —CH=), 7.70 (1H, d, J = 8.0 Hz, H_{Ar}), 7.66–7.63 (2H, m, H_{Ar}), 7.60 (1H, t, J = 7 Hz, H_{Ar}), 7.59 (1H, t, J = 7.0 Hz, H_{Ar}), 7.51 (1H, t, J = 7.5 Hz, H_{Ar}), 7.48 (1H, t, J = 7.5 Hz, H_{Ar}), 2.40 (3H, s, —CH_3), 2.06 (3H, s, —CH_3). LC-MS (*m*/*z*) $[M+H]^+$ calcd for $C_{17}H_{13}ClN_3O_3$ 342.0640, found 342.0728.

4-(4-Chlorobenzylidene)-3-methyl-1-(4-nitrophenyl)pyrazol-5(4H)-one ***(3b)***: orange solid, yield 85%, mp 270–272 °C. IR (ν, cm^{-1}): 3122.3 (C—H), 1701.2 (C=O), 1618.8 (C=N), 1591.2 (C=C). ^1H NMR (500 MHz, DMSO d_6, δ ppm): 8.54 (2H, d, J = 8.0 Hz, H_{Ar}), 8.31 (2H, d, J = 9.0 Hz, H_{Ar}), 8.20 (2H, d, J = 9.0 Hz, H_{Ar}), 7.89 (1H, s, —CH=), 7.63 (2H, d, J = 8.5 Hz, H_{Ar}), 2.39 (3H, s, —CH_3). ^{13}C NMR (125 MHz, DMSO d_6, δ ppm): 161.7, 153.0, 147.2, 143.0, 142.8, 137.8, 134.7, 131.1, 128.3, 126.1, 124.3, 117.4, 12.5. LC-MS (*m*/*z*) $[M-H]^-$ calcd for $C_{17}H_{11}ClN_3O_3$ 340.0494, found 340.0477.

4-(2-Chloro-6-fluorobenzylidene)-3-methyl-1-(4-nitrophenyl)pyrazol-5(4H)-one ***(3c)***: brown solid, yield 84%, mp 230–232 °C. IR (ν, cm^{-1}): 3099.6 (C—H), 1708.9 (C=O), 1641.4 (C=N), 1527.6 (C=C). ^1H NMR (500 MHz, DMSO d_6, δ ppm): 8.36 (2H, d, J = 9.5 Hz, H_{Ar}), 8.31 (2H, d, J = 9.5 Hz, H_{Ar}), 8.15 (2H, d, J = 9.5 Hz, H_{Ar}), 8.10 (2H, d, J = 9.5 Hz, H_{Ar}), 7.91 (1H, s, —CH=), 7.87 (1H, s, —CH=), 7.65–7.62 (1H, m, H_{Ar}), 7.61–7.55 (2H, m, H_{Ar}), 7.49 (1H, d, J = 8.0 Hz, H_{Ar}), 7.46 (1H, d, J = 8.0 Hz, H_{Ar}), 7.37 (1H, t, J = 9.0 Hz, H_{Ar}), 2.42 (1H, s, —CH_3), 1.98 (1H, s, —CH_3). ^{13}C NMR (125 MHz, DMSO d_6, δ ppm): 160.8, 158.3, 153.4, 146.9, 143.3, 142.5, 132.9, 131.2, 129.1, 126.5, 125.6, 122.3, 118.2, 114.5, 12.7. LC-MS (*m*/*z*) $[M+H]^+$ calcd for $C_{17}H_{12}ClFN_3O_3$ 360.0546, found 360.0552.

4-(2,4-Dichlorobenzylidene)-3-methyl-1-(4-nitrophenyl)pyrazol-5(4H)-one ***(3d)***: yellow solid, yield 75%, mp 214–216 °C. ^1H NMR (500 MHz, DMSO d_6, δ ppm): 8.53 (1H, d, J = 8.5 Hz, H_{Ar}), 8.29 (2H, d, J = 9.5 Hz, H_{Ar}), 8.15 (2H, d, J = 9.5 Hz, H_{Ar}), 8.12–7.97 (1H, m, H_{Ar}), 7.91 (1H, s, —CH=), 7.59–7.56 (1H, m, H_{Ar}), 2.39 (3H, s, —CH_3). LC-MS (*m*/*z*) $[M+H]^+$ calcd for $C_{17}H_{12}N_3O_3Cl_2$ 376.0250, found 376.0475.

4-(3,4-Dichlorobenzylidene)-3-methyl-1-(4-nitrophenyl)pyrazol-5(4H)-one ***(3e)***: red solid, yield 75%, mp 277–278 °C. IR (ν, cm^{-1}): 3118.6 (C—H), 1707.4 (C=O), 1621.8 (C=N), 1591.7 (C=C). ^1H NMR (500 MHz, DMSO d_6, δ ppm): 8.89 (1H, d, J = 2.0 Hz, H_{Ar}), 8.39 (1H, dd, J = 8.5, 2.0 Hz, H_{Ar}), 8.31 (2H, d, J = 9.5 Hz, H_{Ar}), 8.19 (2H, d, J = 9.5 Hz, H_{Ar}), 7.88 (1H, s, —CH=), 7.82 (1H, d, J = 8.5 Hz, H_{Ar}), 2.38 (3H, s, —CH_3). ^{13}C NMR (125 MHz, DMSO d_6, δ ppm): 159.8, 152.6, 146.5, 143.4, 142.2, 134.9, 133.5, 132.1, 130.3, 129.7, 127.9, 127.2, 126.3, 117.9, 12.8. LC-MS (*m*/*z*) $[M+H]^+$ calcd for $C_{17}H_{12}N_3O_3Cl_2$ 376.0250, found 376.0475.

4-(2,4-Dimethoxybenzylidene)-3-methyl-1-(4-nitrophenyl)pyrazol-5(4H)-one ***(3f)***: yellow solid, yield 85%, mp 232–234 °C. IR (ν, cm^{-1}): 3130.5 (C—H), 1697.4 (C=O), 1602.9 (C=N), 1521.8 (C=C). ^1H NMR (500 MHz, DMSO d_6, δ ppm): 9.24 (1H, d, J = 8.5 Hz, H_{Ar}), 8.28 (2H, d, J = 9.5 Hz, H_{Ar}), 8.22 (2H, d, J = 9.5 Hz, H_{Ar}), 8.01 (1H, s, —CH=), 6.73 (1H, d, J = 2.0 Hz, H_{Ar}), 6.71 (1H, dd, J = 8.0, 2.0 Hz, H_{Ar}), 3.98 (3H, s, —OCH_3), 3.94 (3H, s, —OCH_3), 2.33 (3H, s, —CH_3). LC-MS (*m*/*z*) $[M+H]^+$ calcd for $C_{19}H_{18}N_3O_5$ 368.1241, found 368.1247.

4-(2,5-Dimethoxybenzylidene)-3-methyl-1-(4-nitrophenyl)pyrazol-5(4H)-one ***(3g)***: red solid, yield 86%, mp 233–234 °C. IR (ν, cm^{-1}): 3124.7 (C—H), 1674.2 (C=O), 1598.9 (C=N), 1531.5 (C=C). ^{1}H NMR (500 MHz, DMSO d_6, δ ppm): 8.71 (1H, d, J = 3.0 Hz, H_{Ar}), 8.33 (2H, d, J = 9.5 Hz, H_{Ar}), 8.21 (2H, d, J = 9.5 Hz, H_{Ar}), 8.05 (1H, s, —CH=), 7.27 (1H, dd, J = 9.0, 2.5 Hz, H_{Ar}), 7.15 (1H, d, J = 9.5 Hz, H_{Ar}), 3.90 (3H, s, —OCH_3), 3.81 (3H, s, —OCH_3), 2.35 (3H, s, —CH_3). LC-MS (m/z) $[M+H]^+$ calcd for $C_{19}H_{18}N_3O_5$ 368.1241, found 368.1247.

4-(3,4-Dimethoxybenzylidene)-3-methyl-1-(4-nitrophenyl)pyrazol-5(4H)-one ***(3h)***: yellow solid, yield 80%, mp 241–242 °C. IR (ν, cm^{-1}): 3074.8 (C—H), 1680.8 (C=O), 1591.1 (C=N), 1565.0 (C=C). ^{1}H NMR (500 MHz, DMSO d_6, δ ppm): 8.76 (1H, s, H_{Ar}), 8.34 (2H, d, J = 9.0 Hz, H_{Ar}), 8.24 (2H, d, J = 9.0 Hz, H_{Ar}), 8.11 (1H, d, J = 9.0 Hz, H_{Ar}), 7.85 (1H, s, —CH=), 7.21 (1H, d, J = 8.5 Hz, H_{Ar}), 3.91 (3H, s, —OCH_3), 3.89 (3H, s, —OCH_3), 2.37 (3H, s, —CH_3). LC-MS (m/z) $[M + Na]^+$ calcd for $C_{19}H_{17}N_3O_5Na$ 390.1060, found 390.0924.

4-(4-(Dimethylamino)benzylidene)-3-methyl-1-(4-nitrophenyl)pyrazol-5(4H)-one ***(3i)***: red solid, yield 80%, mp 143–144 °C. IR (ν, cm^{-1}): 3445.2 (N-H), 3073.5 (C—H), 1677.0 (C=O), 1553.4 (C=C). ^{1}H NMR (500 MHz, DMSO d_6, δ ppm): 8.62 (2H, d, J = 8.5 Hz, H_{Ar}), 8.31–8.26 (4H, m, H_{Ar}), 7.64 (1H, s, —CH=), 6.87 (2H, d, J = 9.0 Hz, H_{Ar}), 3.15 (6H, s, -N(CH_3)$_2$), 2.33 (3H, s, —CH_3). ^{13}C NMR (125 MHz, DMSO d_6, δ ppm): 162.8, 154.0, 153.1, 148.6, 143.7, 142.4, 137.2, 124.3, 120.9, 117.5, 117.0, 111.1, 12.6. LC-MS (m/z) $[M + Na]^+$ calcd for $C_{19}H_{18}N_4O_3Na$ 373.1271, found 373.1272.

4-(4-Ethoxybenzylidene)-3-methyl-1-(4-nitrophenyl)pyrazol-5(4H)-one ***(3j)***: yellow solid, yield 85%, mp 208–209 °C. IR (ν, cm^{-1}): 3125.2 (C—H), 1689.3 (C=O), 1590.2 (C=C). ^{1}H NMR (500 MHz, DMSO d_6, δ ppm): 8.63 (2H, d, J = 9.0 Hz, H_{Ar}), 8.27 (2H, d, J = 9.5 Hz, H_{Ar}), 8.19 (2H, d, J = 9.0 Hz, H_{Ar}), 7.77 (1H, s, —CH=), 7.09 (2H, d, J = 9.0 Hz, H_{Ar}), 4.16 (2H, q, J = 7.0 Hz, —OCH_2—), 2.33 (3H, s, —CH_3), 1.36 (3H, t, J = 7.0 Hz, —CH_3). ^{13}C NMR (125 MHz, DMSO d_6, δ ppm): 163.4, 162.6, 153.8, 149.4, 143.4, 142.8, 137.2, 125.9, 124.9, 122.6, 117.4, 114.8, 64.0, 14.4, 13.2. LC-MS (m/z) $[M + Na]^+$ calcd for $C_{19}H_{17}N_3O_4Na$ 374.1111, found 374.1089.

4-(3-Ethoxy-4-hydroxybenzylidene)-3-methyl-1-(4-nitrophenyl)pyrazol-5(4H)-one ***(3k)***: yellow solid, yield 51%, mp 214–215 °C. IR (ν, cm^{-1}): 3078.6 (O-H), 1672.4 (C=O), 1588.3 (C=N), 1566.1 (C=C). ^{1}H NMR (500 MHz, DMSO d_6, δ ppm): 10.60 (1H, s, —OH), 8.73 (1H, s, H_{Ar}), 8.33 (2H, d, J = 9.5 Hz, H_{Ar}), 8.24 (2H, d, J = 9.0 Hz, H_{Ar}), 8.00 (1H, d, J = 7.5 Hz, H_{Ar}), 7.76 (1H, s, —CH=), 6.98 (1H, d, J = 8.5 Hz, H_{Ar}), 4.16 (2H, q, J = 7.0 Hz, —OCH_2—), 2.36 (3H, s, —CH_3), 1.42 (3H, t, J = 7.0 Hz, —CH_3). ^{13}C NMR (125 MHz, DMSO d_6, δ ppm): 162.8, 153.83, 153.79, 150.3, 146.5, 142.8, 142.5, 131.6, 125.2, 125.0, 121.4, 118.2, 117.5, 115.8, 63.9, 14.6, 13.2. LC-MS (m/z) $[M-H]^-$ calcd for $C_{19}H_{16}N_3O_5$ 366.1095, found 366.1054.

4-(4-Fluorobenzylidene)-3-methyl-1-(4-nitrophenyl)pyrazol-5(4H)-one ***(3l)***: yellow solid, yield 86%, mp 284–285 °C. IR (ν, cm^{-1}): 3130.9 (C—H), 1693.0 (C=O), 1625.9 (C=N), 1594.3 (C=C). ^{1}H NMR (500 MHz, DMSO d_6, δ ppm): 8.69 (2H, d, J = 8.5 Hz, H_{Ar}), 8.34 (2H, d, J = 9.0 Hz, H_{Ar}), 8.22 (2H, d, J = 9.0 Hz, H_{Ar}), 7.95 (1H, s, —CH=), 7.45 (2H, t, J = 9.0 Hz, H_{Ar}), 2.39 (3H, s, —CH_3). ^{13}C NMR (125 MHz, DMSO d_6, δ ppm): 161.9, 153.1, 147.6, 142.9, 142.8, 136.3, 136.2, 125.2, 124.4, 117.4, 115.5, 115.3, 12.6. LC-MS (m/z) $[M+H]^+$ calcd for $C_{17}H_{13}FN_3O_3$ 326.0935, found 326.2197.

4-(3-Hydroxybenzylidene)-3-methyl-1-(4-nitrophenyl)pyrazol-5(4H)-one ***(3m)***: yellow solid, yield 77%, mp 255–256 °C. IR (ν, cm^{-1}): 3121.9 (C—H), 1692.1 (C=O), 1592.3 (C=N). ^{1}H NMR (500 MHz, DMSO d_6, δ ppm): 9.84 (1H, s, —OH), 8.32 (2H, d, J = 9.0 Hz, H_{Ar}), 8.20 (2H, d, J = 9.5 Hz, H_{Ar}), 8.12 (1H, s, H_{Ar}), 7.90 (1H, d, J = 7.5 Hz, H_{Ar}), 7.80 (1H, s, —CH=), 7.38 (1H, t, J = 8.0 Hz, H_{Ar}), 7.06 (1H, dd, J = 8.0, 2.0 Hz, H_{Ar}), 2.37 (3H, s, —CH_3). ^{13}C NMR (125 MHz, DMSO d_6, δ ppm): 162.1, 157.3, 153.7, 150.0, 143.2, 142.9, 133.9, 129.8, 129.6, 126.4, 125.6, 125.5, 125.1, 125.0, 121.1, 119.7, 117.4, 117.2, 17.5, 13.2. LC-MS (m/z) $[M-H]^-$ calcd for $C_{17}H_{12}N_3O_4$ 322.0833, found 322.0879.

4-(4-Hydroxybenzylidene)-3-methyl-1-(4-nitrophenyl)pyrazol-5(4H)-one ***(3n)***: yellow solid, yield 78%, mp 301–303 °C. IR (ν, cm^{-1}): 3344.6 (O-H), 3112.9 (C—H), 1669.1 (C=O), 1590.7 (C=N), 1564.7 (C=C). ^{1}H NMR (500 MHz, DMSO d_6, δ ppm): 10.95 (1H, s, —OH), 8.61 (2H, d, J = 8.5 Hz, H_{Ar}), 8.31 (2H, d, J = 9.5 Hz, H_{Ar}), 8.23 (2H, d, J = 9.5 Hz, H_{Ar}), 7.78 (1H, s, —CH=), 6.96 (2H, d, J = 8.5 Hz, H_{Ar}), 2.36 (3H, s, —CH_3). ^{13}C NMR (125 MHz, DMSO d_6, δ ppm): 163.6, 162.7, 153.9, 149.9, 143.5, 142.7, 137.7, 125.0, 124.8, 121.5, 117.4, 116.0, 13.2. LC-MS (m/z) $[M-H]^-$ calcd for $C_{17}H_{12}N_3O_4$ 322.0833, found 322.0857.

4-(3-Hydroxy-4-methoxybenzylidene)-3-methyl-1-(4-nitrophenyl)pyrazol-5(4H)-one ***(3o)***: yellow solid, yield 57%, mp 281–282 °C. IR (ν, cm^{-1}): 3422.4 (C—H), 1672.4 (C=O), 1588.3 (C=N), 1566.1 (C=C). ^{1}H NMR (500 MHz, DMSO d_6, δ ppm): 9.49 (1H, s, —OH), 8.39 (1H, d, J = 2.0 Hz, H_{Ar}), 8.30 (2H, d, J = 9.0 Hz, H_{Ar}), 8.21 (2H, d, J = 9.0 Hz, H_{Ar}), 8.02 (1H, dd, J = 8.5, 2.0 Hz, H_{Ar}), 7.70 (1H, s, —CH=), 7.13 (1H, d, J = 8.5 Hz, H_{Ar}), 3.92 (3H, s, —OCH_3), 2.34 (3H, s, —CH_3). ^{13}C NMR (125 MHz, DMSO d_6, δ ppm): 162.6, 153.8, 153.5, 150.1, 146.2, 143.5, 142.7, 129.7, 126.3, 125.1, 124.9, 122.4, 120.0, 117.4, 111.6, 55.9, 13.2. LC-MS (m/z) $[M-H]^-$ calcd for $C_{18}H_{14}N_3O_5$ 352.0939, found 352.0681.

4-(3-Methoxybenzylidene)-3-methyl-1-(4-nitrophenyl)pyrazol-5(4H)-one ***(3p)***: yellow solid, yield 71%, mp 188–190 °C. IR (ν, cm^{-1}): 3116.2 (C—H), 1699.0 (C=O), 1619.8 (C=N), 1593.2 (C=C). ^{1}H NMR (500 MHz, DMSO d_6, δ ppm): 8.39 (1H, s, H_{Ar}), 8.33 (2H, d, J = 9.0 Hz, H_{Ar}), 8.19 (2H, d, J = 9.0 Hz, H_{Ar}), 8.01 (1H, d, J = 7.5 Hz, H_{Ar}), 7.87 (1H, s, —CH=), 7.49 (1H, t, J = 8.0 Hz, H_{Ar}), 7.23 (1H, dd, J = 8.5, 2.0 Hz, H_{Ar}), 3.86 (3H, s, —OCH_3), 2.37 (3H, s, —CH_3). ^{13}C NMR (125 MHz, DMSO d_6, δ ppm): 161.8, 158.9, 153.1, 148.9, 142.9, 142.8, 133.5, 129.1, 126.3, 125.7, 124.5, 124.3, 119.5, 117.6, 117.4, 117.1, 55.1, 12.6. LC-MS (m/z) $[M + Na]^+$ calcd for $C_{18}H_{15}N_3O_4Na$ 360.0955, found 360.0435.

4-(4-Methoxybenzylidene)-3-methyl-1-(4-nitrophenyl)pyrazol-5(4H)-one ***(3q)***: red solid, yield 75%, mp 229–231 °C. IR (ν, cm^{-1}): 3124.7 (C—H), 1687.7 (C=O), 1579.7 (C=N), 1508.3 (C=C). ^{1}H NMR (500 MHz, DMSO d_6, δ ppm): 8.68 (2H, d, J = 8.5 Hz, H_{Ar}), 8.32 (2H, d, J = 9.0 Hz, H_{Ar}), 8.23 (2H, d, J = 9.5 Hz, H_{Ar}), 7.85 (1H, s, —CH=), 7.16 (2H, d, J = 8.5 Hz, H_{Ar}), 3.91 (3H, s, —OCH_3), 2.37 (s, 3H, —CH_3). LC-MS (m/z) $[M+H]^+$ calcd for $C_{18}H_{16}N_3O_4$ 338.1135, found 338.1141.

3-Methyl-4-(4-(methylthio)benzylidene)-1-(4-nitrophenyl)pyrazol-5(4H)-one ***(3r)***: yellow solid, yield 80%, mp 217–220 °C. IR (ν, cm^{-1}): 3109.3 (C—H), 1678.1 (C=O), 1608.6 (C=N), 1523.8 (C=C). ^{1}H NMR (500 MHz, DMSO d_6, δ ppm): 8.57 (2H, d, J = 8.5 Hz, H_{Ar}), 8.32 (2H, d, J = 9.0 Hz, H_{Ar}), 8.22 (2H, d, J = 9.5 Hz, H_{Ar}), 7.85 (1H, s, —CH=), 7.45 (2H, d, J = 9.0 Hz, H_{Ar}), 2.59 (3H, s, -SCH_3), 2.37 (3H, s, —CH_3). ^{13}C NMR (125 MHz, DMSO d_6, δ ppm): 160.3, 153.1, 146.6, 143.1, 142.2, 138.7, 129.6, 128.9, 128.5, 126.8, 126.2, 118.0, 13.7, 12.6. LC-MS (m/z) $[M+H]^+$ calcd for $C_{18}H_{16}N_3O_3S$ 354.0907, found 354.0913.

3-Methyl-4-(3-nitrobenzylidene)-1-(4-nitrophenyl)pyrazol-5(4H)-one ***(3s)***: red solid, yield 85%, mp 268–269 °C. IR (ν, cm^{-1}): 3090.8 (C—H), 1690.6 (C=O), 1589.9 (C=N). ^{1}H NMR (500 MHz, DMSO d_6, δ ppm): 9.54 (1H, s, H_{Ar}), 8.79 (1H, d, J = 8 Hz, H_{Ar}), 8.44 (1H, dd, J = 8.5, 1.5 Hz, H_{Ar}), 8.33 (2H, d, J = 9 Hz, H_{Ar}), 8.19 (2H, d, J = 9.5 Hz, H_{Ar}), 8.09 (1H, s, —CH=), 7.87 (1H, t, J = 8.5 Hz, H_{Ar}), 2.40 (3H, s, —CH_3). LC-MS (m/z) $[M+H]^+$ calcd for $C_{17}H_{13}N_4O_5$ 353.0881, found 353.1984.

3-Methyl-4-(4-nitrobenzylidene)-1-(4-nitrophenyl)pyrazol-5(4H)-one ***(3t)***: red solid, yield 65%, mp 285–286 °C. ^{1}H NMR (500 MHz, DMSO d_6, δ ppm): 8.65 (2H, d, J = 9.0 Hz, H_{Ar}), 8.38 (2H, d, J = 8.5 Hz, H_{Ar}), 8.34 (2H, d, J = 9.5 Hz, H_{Ar}), 8.18 (2H, d, J = 9.5 Hz, H_{Ar}), 8.06 (1H, s, —CH=), 2.40 (3H, s, —CH_3). LC-MS (m/z) $[M+H]^+$ calcd for $C_{17}H_{13}N_4O_5$ 353.0881, found 353.1833.

3-Methyl-1-(4-nitrophenyl)-4-(2,4,5-trimethoxybenzylidene)pyrazol-5(4H)-one ***(3u)***: red solid, yield 82%, mp 219–220 °C. IR (ν, cm^{-1}): 3114.8 (C—H), 1702.1 (C=O), 1594.7 (C=N), 1504.8 (C=C). ^{1}H NMR (500 MHz, DMSO d_6, δ ppm): 8.34–8.29 (4H, m, H_{Ar}), 8.19–8.14 (4H, m, H_{Ar}), 7.76 (1H, s, —CH=), 7.69 (1H, s, —CH=), 6.36 (2H, s, H_{Ar}), 6.32 (2H, s, H_{Ar}), 3.895 (3H, s, —OCH_3), 3.892 (3H, s, —OCH_3), 3.85 (6H, s, —OCH_3), 3.82 (6H, s, —OCH_3), 2.33 (3H, s, —CH_3), 2.06 (3H, s, —CH_3). ^{13}C NMR (125 MHz, DMSO d_6, δ ppm): 164.83, 164.77, 163.9, 161.3, 160.7, 159.7, 151.9, 150.9, 143.3, 142.82, 142.79, 142.4, 138.4, 138.2, 126.2, 124.7, 124.43, 124.36, 116.9, 116.6, 104.7, 104.1, 91.0, 90.6, 55.7, 55.6, 55.4, 55.3, 14.2, 12.5. LC-MS (m/z) $[M + Na]^+$ calcd for $C_{20}H_{19}N_3O_6Na$ 420.1166, found 420.1107.

4-(Benzo[d][1,3]dioxol-5-ylmethylene)-3-methyl-1-(4-nitrophenyl)pyrazol-5(4H)-one ***(3v)***: yellow solid, yield 80%, mp 261–263 °C. IR (ν, cm^{-1}): 3092.4 (C—H), 1691.8 (C=O), 1592.7 (C=N), 1574.0 (C=C). ^{1}H NMR (500 MHz, DMSO d_6, δ ppm): 8.66 (1H, s, H_{Ar}), 8.32 (2H, d, J = 9.5 Hz, H_{Ar}), 8.23 (2H, d, J = 9.0 Hz, H_{Ar}), 8.01 (1H, d, J = 8.5 Hz, H_{Ar}), 7.83 (1H, s, —CH=), 7.18 (1H, d, J = 8.0 Hz, H_{Ar}), 6.22 (2H, s, —OCH_2O-), 2.36 (3H, s, —CH_3). ^{13}C NMR (125 MHz, DMSO d_6, δ ppm): 162.2, 153.2, 152.1, 148.9, 147.4, 143.0, 142.9, 132.5, 127.2, 124.3, 122.9, 117.4, 111.6, 108.2, 102.0, 12.6. LC-MS (m/z) $[M + Na]^+$ calcd for $C_{18}H_{13}N_3O_5Na$ 374.0747, found 374.0935.

4-(Furan-2-ylmethylene)-3-methyl-1-(4-nitrophenyl)pyrazol-5(4H)-one ***(3w)***: brown solid, yield 84%, mp 207–209 °C. IR (ν, cm^{-1}): 3126.6 (C—H), 1687.7 (C=O), 1618.3 (C=N), 1523.8 (C=C). ^{1}H NMR (500 MHz, DMSO d_6, δ ppm): 8.61 (1H, d, J = 4.0 Hz, H_{Ar}), 8.34 (2H, d, J = 9.0 Hz, H_{Ar}), 8.33 (2H, d, J = 9.5 Hz, H_{Ar}), 8.32 (1H, d, J = 4.0 Hz, H_{Ar}), 8.30 (1H, d, J = 4.0 Hz, H_{Ar}), 8.22 (2H, d, J = 9.0 Hz, H_{Ar}), 8.19 (2H, d, J = 9.0 Hz, H_{Ar}), 7.78 (1H, s, —CH=), 7.70 (1H, d, J = 3.5 Hz, H_{Ar}), 7.62 (1H, s, —CH=), 6.97 (1H, dd, J = 4.0, 1.0 Hz, H_{Ar}), 6.91 (1H, dd, J = 4.0, 1.5 Hz, H_{Ar}), 2.51 (3H, s, —CH_3), 2.36 (3H, s, —CH_3). LC-MS (m/z) $[M+H]^+$ calcd for $C_{15}H_{12}N_3O_4$ 298.0822, found 298.0828.

3-Methyl-1-(4-nitrophenyl)-4-(pyridin-3-ylmethylene)pyrazol-5(4H)-one ***(3x)***: yellow solid, yield 79%, mp 230–232 °C. IR (ν, cm^{-1}): 3120.8 (C—H), 1695.4 (C=O), 1591.3 (C=N), 1496.8 (C=C). ^{1}H NMR (500 MHz, DMSO d_6, δ ppm): 9.37 (1H, s, H_{Ar}), 9.06 (1H, d, J = 8.0 Hz, H_{Ar}), 8.75 (1H, d, J = 4.5 Hz, H_{Ar}), 8.34 (2H, d, J = 9.0 Hz, H_{Ar}), 8.20 (2H, d, J = 9.0 Hz, H_{Ar}), 7.99 (1H, s, —CH=), 7.63–7.61 (1H, m, H_{Ar}), 2.50 (3H, s, —CH_3). ^{13}C NMR (125 MHz, DMSO d_6, δ ppm): 160.0, 152.4, 149.4, 148.2, 145.9, 142.3, 141.6, 132.8, 132.4, 128.2, 125.5, 123.7, 117.4, 13.1. LC-MS (m/z) $[M+H]^+$ calcd for $C_{16}H_{13}N_4O_3$ 309.0982, found 309.0988.

*General procedure for the synthesis of 4-(arylmethyl)-1-aryl-3-methyl-1H-pyrazol-5-ol (****4a-4p, 5a-5h****).*

Pyrazol-5(4*H*)-one derivatives (**2** and **3**, 0.01 mol) were dissolved in 100 mL of absolute ethanol and cooled to 0–5 °C. The mixture was added $NaBH_4$ (0.01 mol) and stirred for 30 min. After completion, the reaction mixture was neutralized with HCl 10% to pH = 7, allowed to cool, filtered, and poured on crushed ice. Solids precipitated were filtered and recrystallized using ethanol (Scheme 1). All compounds have high purity which was assessed by a high resolution of ^{1}H NMR (500 MHz).

4-(2-Chlorobenzyl)-3-methyl-1-(3-nitrophenyl)-1H-pyrazol-5-ol ***(4a)***: red solid, yield 84%, mp 191–193 °C. IR (ν, cm^{-1}): 3090.8 (=C—H), 1622.1 (C=C), 1525.7 and 1344.4 (NO_2). ^{1}H NMR (500 MHz, DMSO d_6, δ ppm): 11.50 (1H, brs, —OH), 8.68 (1H, t, J = 2.0 Hz, H_{Ar}), 8.23 (1H, dd, J = 8.5, 1.5 Hz, H_{Ar}), 8.02 (1H, dd, J = 8.5, 2.0 Hz, H_{Ar}), 7.73 (1H, t, J = 8.5 Hz, H_{Ar}), 7.42 (1H, dd, J = 7.5, 1.5 Hz, H_{Ar}), 7.27–7.19 (3H, m, H_{Ar}), 3.34 (2H, s, —CH_2—), 2.05 (3H, s, —CH_3). ^{13}C NMR (125 MHz, DMSO d_6, δ ppm): 155.2, 149.7, 148.1, 139.0, 137.4, 135.8, 132.8, 130.4, 129.9, 129.0, 127.7, 127.1, 124.3, 118.6, 112.7, 25.1, 12.0. LC-MS (m/z) $[M-H]^-$ calcd for $C_{17}H_{13}ClN_3O_3$ 342.0651, found 342.0612.

4-(4-Chlorobenzyl)-3-methyl-1-(3-nitrophenyl)-1H-pyrazol-5-ol ***(4b)***: red solid, yield 82%, mp 230–232 °C. IR (ν, cm^{-1}): 3130.5 (=C—H), 1685.8 (C=O), 1612.5 (C=C), 1523.8 (NO_2). ^{1}H NMR (500 MHz, DMSO d_6, δ ppm): 11.12 (1H, brs, —OH), 8.67 (1H, s, H_{Ar}), 8.22 (1H, d, J = 7.5 Hz, H_{Ar}), 8.03 (1H, dd, J = 8.0, 1.5 Hz, H_{Ar}), 7.72 (1H, t, J = 8.0 Hz, H_{Ar}), 7.32 (2H, d, J = 8.5 Hz, H_{Ar}), 7.25 (2H, d, J = 8.0 Hz, H_{Ar}), 3.63 (2H, s, —CH_2—), 2.09 (3H, s, —CH_3). ^{13}C NMR (125 MHz, DMSO d_6, δ ppm): 157.3, 153.4, 148.1, 139.7, 138.7, 135.8, 132.2, 130.5, 130.4, 129.9, 128.2, 119.4, 112.8, 26.6, 13.2. LC-MS (m/z) $[M-H]^-$ calcd for $C_{17}H_{13}ClN_3O_3$ 342.0651, found 342.0612.

4-(2-Chloro-6-fluorobenzyl)-3-methyl-1-(3-nitrophenyl)-1H-pyrazol-5-ol ***(4c)***: red solid, yield 79%, mp 189–190 °C. IR (ν, cm^{-1}): 3120.8 (=C—H), 2870.1 (C—H), 1525.7 và 1342.5 (NO_2). ^{1}H NMR (500 MHz, DMSO d_6, δ ppm): 11.05 (1H, brs, —OH), 8.63 (1H, s, H_{Ar}), 8.17 (1H, d, J = 8.0 Hz, H_{Ar}), 8.01 (1H, d, J = 7.0 Hz, H_{Ar}), 7.72 (1H, t, J = 8.0 Hz, H_{Ar}), 7.31–7.28 (2H, m, H_{Ar}), 7.19–7.17 (1H, m, H_{Ar}), 3.74 (2H, s, —CH_2—), 1.98 (3H, s, —CH_3). ^{13}C NMR (125 MHz, DMSO d_6, δ ppm): 154.7, 149.2, 148.1, 139.1, 138.5, 134.5, 134.4, 130.5, 128.9, 128.8, 127.1, 125.4, 118.6, 114.4, 114.2, 26.1, 13.2. LC-MS (m/z) $[M-H]^-$ calcd for $C_{17}H_{12}ClFN_3O_3$ 360.0557, found 360.0516.

4-(3,4-Dichlorobenzyl)-3-methyl-1-(3-nitrophenyl)-1H-pyrazol-5-ol ***(4d)***: red solid, yield 82%, mp 277–278 °C. IR (ν, cm^{-1}): 3076.5 (═C─H), 2908.7 (C─H), 1525.7 and 1344.4 (NO_2). ^{1}H NMR (500 MHz, DMSO d_6, δ ppm): 11.25 (1H, brs, ─OH), 8.66 (1H, s, H_{Ar}), 8.22 (1H, d, J = 8.5 Hz, H_{Ar}), 8.03 (1H, dd, J = 8.0, 1.5 Hz, H_{Ar}), 7.73 (1H, t, J = 8.5 Hz, H_{Ar}), 7.53 (1H, d, J = 8.0 Hz, H_{Ar}), 7.48 (1H, s, H_{Ar}), 7.23 (1H, d, J = 8.0 Hz, H_{Ar}), 3.64 (2H, s, ─CH_2─), 2.12 (3H, s, ─CH_3). ^{13}C NMR (125 MHz, DMSO d_6, δ ppm): 154.2, 148.2, 148.1, 138.1, 137.2, 135.2, 133.2, 130.7, 130.5, 130.4, 129.9, 128.5, 128.4, 118.7, 113.2, 26.4, 12.1. LC-MS (m/z) [M−H]$^-$ calcd for $C_{17}H_{12}Cl_2N_3O_3$ 376.0261, found 376.0237.

4-(2,4-Dimethoxybenzyl)-3-methyl-1-(3-nitrophenyl)-1H-pyrazol-5-ol ***(4e)***: red solid, yield 84%, mp 194–196 °C. IR (ν, cm^{-1}): 3203.8 (═C─H), 1527.6 and 1346.3 (NO_2). ^{1}H NMR (500 MHz, DMSO d_6, δ ppm): 11.19 (1H, brs, ─OH), 8.67 (1H, s, H_{Ar}), 8.21 (1H, d, J = 7.5 Hz, H_{Ar}), 8.01 (1H, d, J = 7.5 Hz, H_{Ar}), 7.72 (1H, t, J = 8.0 Hz, H_{Ar}), 6.66 (1H, d, J = 8.5 Hz, H_{Ar}), 6.52 (1H, s, H_{Ar}), 6.42 (1H, dd, J = 8.5, 1.5 Hz, H_{Ar}), 3.80 (3H, s, ─OCH_3), 3.72 (3H, s, ─OCH_3), 3.31 (2H, s, ─CH_2─), 2.08 (3H, s, ─CH_3). ^{13}C NMR (125 MHz, DMSO d_6, δ ppm): 158.9, 157.7, 148.1, 138.7, 138.2, 135.1, 134.8, 131.0, 130.8, 130.4, 129.2, 128.4, 128, 118.1, 113.2, 55.2, 55.1, 26.6, 14.0. LC-MS (m/z) [M−H]$^-$ calcd for $C_{19}H_{18}N_3O_5$ 368.1252, found 368.1192.

4-(3,4-Dimethoxybenzyl)-3-methyl-1-(3-nitrophenyl)-1H-pyrazol-5-ol ***(4f)***: red solid, yield 81%, mp 208–210 °C. IR (ν, cm^{-1}): 3088.0 (═C─H), 2918.3 (C─H), 1525.7 and 1344.4 (NO_2). ^{1}H NMR (500 MHz, DMSO d_6, δ ppm): 11.05 (1H, brs, ─OH), 8.66 (1H, s, H_{Ar}), 8.22 (1H, d, J = 8.0 Hz, H_{Ar}), 8.02 (1H, d, J = 7.5 Hz, H_{Ar}), 7.72 (1H, t, J = 8.5 Hz, H_{Ar}), 6.85 (1H, d, J = 9.0 Hz, H_{Ar}), 6.83 (1H, s, H_{Ar}), 6.72 (1H, t, J = 7.5 Hz, H_{Ar}), 3.71 (3H, s, ─OCH_3), 3.70 (3H, s, ─OCH_3), 3.31 (2H, s, ─CH_2─), 2.09 (3H, s, ─CH_3). ^{13}C NMR (125 MHz, DMSO d_6, δ ppm): 155.2, 148.6, 148.1, 138.6, 138.22, 135.8, 133.1, 130.5, 130.1, 129.9, 129.7, 128.0, 127.2, 119.8, 112.3, 55.6, 55.4, 26.8, 14.0. LC-MS (m/z) [M−H]$^-$ calcd for $C_{19}H_{18}N_3O_5$ 368.1252, found 368.1192.

4-(4-Fluorobenzyl)-3-methyl-1-(3-nitrophenyl)-1H-pyrazol-5-ol ***(4g)***: red solid, yield 87%, mp 179–180 °C. IR (ν, cm^{-1}): 3240.4 (═C─H), 2918.3 (C─H), 1523.2 and 1342.5 (NO_2). ^{1}H NMR (500 MHz, DMSO d_6, δ ppm): 11.10 (1H, brs, ─OH), 8.67 (1H, s, H_{Ar}), 8.21 (1H, d, J = 8.0 Hz, H_{Ar}), 8.02 (1H, dd, J = 8.5, 1.5 Hz, H_{Ar}), 7.73 (1H, t, J = 8.5 Hz, H_{Ar}), 7.26 (2H, dd, J = 7.0, 5.5 Hz, H_{Ar}), 7.08 (2H, t, J = 9.0 Hz, H_{Ar}), 3.62 (2H, s, ─CH_2─), 2.08 (3H, s, ─CH_3). ^{13}C NMR (125 MHz, DMSO d_6, δ ppm): 161.5, 159.6, 148.1, 139.7, 138.7, 135.8, 132.2, 130.5, 130.4, 129.9, 128.2, 119.4, 112.8, 26.4, 13.1. LC-MS (m/z) [M−H]$^-$ calcd for $C_{17}H_{13}FN_3O_3$ 326.0946, found 326.0901.

4-(2-Hydroxybenzyl)-3-methyl-1-(3-nitrophenyl)-1H-pyrazol-5-ol ***(4h)***: red solid, yield 82%, mp 197–198 °C. IR (ν, cm^{-1}): 3105.4 (═C─H), 1583.2 (C═C), 1518.0 and 1342.5 (NO_2). ^{1}H NMR (500 MHz, DMSO d_6, δ ppm): 10.50 (1H, brs, ─OH), 9.30 (1H, s, ─OH), 8.68 (1H, t, J = 2.0 Hz, H_{Ar}), 8.23 (1H, dd, J = 8.0, 1.5 Hz, H_{Ar}), 8.03 (1H, dd, J = 8.0, 1.5 Hz, H_{Ar}), 7.72 (1H, t, J = 8.5 Hz, H_{Ar}), 7.01–6.98 (2H, m, H_{Ar}), 6.77 (1H, d, J = 7.5 Hz, H_{Ar}), 6.69 (1H, t, J = 7.5 Hz, H_{Ar}), 3.52 (2H, s, ─CH_2─), 2.12 (3H, s, ─CH_3). ^{13}C NMR (125 MHz, DMSO d_6, δ ppm): 153.1, 149.1, 148.7, 139.2, 138.2, 134.1, 133.2, 131.1, 129.2, 129.1, 128.6, 128.0, 125.2, 119.1, 111.3, 23.4, 12.6. LC-MS (m/z) [M−H]$^-$ calcd for $C_{17}H_{14}N_3O_4$ 324.0990, found 324.0951.

4-(4-Hydroxybenzyl)-3-methyl-1-(3-nitrophenyl)-1H-pyrazol-5-ol ***(4i)***: red solid, yield 77%, mp 205–206 °C. IR (ν, cm^{-1}): 3074.6 (═C─H), 2900.9 (C─H), 1583.6 (C═C), 1521.8 and 1344.4 (NO_2). ^{1}H NMR (500 MHz, DMSO d_6, δ ppm): 11.01 (1H, brs, ─OH), 9.11 (1H, s, ─OH), 8.67 (1H, s, H_{Ar}), 8.21 (1H, d, J = 7.5 Hz, H_{Ar}), 8.01 (1H, d, J = 7.5 Hz, H_{Ar}), 7.72 (1H, t, J = 8.5 Hz, H_{Ar}), 7.01 (2H, d, J = 7.5 Hz, H_{Ar}), 6.65 (2H, d, J = 8.5 Hz, H_{Ar}), 3.47 (2H, s, ─CH_2─), 2.08 (3H, s, ─CH_3). ^{13}C NMR (125 MHz, DMSO d_6, δ ppm): 156.3, 151.2, 148.2, 139.8, 138.7, 135.2, 133.3, 130.1, 130.0, 129.8, 128.7, 118.9, 113.1, 24.5, 12.3. LC-MS (m/z) [M−H]$^-$ calcd for $C_{17}H_{14}N_3O_4$ 324.0990, found 324.0951.

4-(3-Hydroxy-4-methoxybenzyl)-3-methyl-1-(3-nitrophenyl)-1H-pyrazol-5-ol ***(4j)***: red solid, yield 84%, mp 208–210 °C. IR (ν, cm^{-1}): 3093.8 (═C─H), 1633.1 (C═C), 1521.8 and 1321.8 (NO_2). ^{1}H NMR (500 MHz, DMSO d_6, δ ppm): 10.92 (1H, brs, ─OH), 8.77 (1H, s, ─OH), 8.70 (1H, s, H_{Ar}), 8.24 (1H, dd, J = 8.5, 1.5 Hz, H_{Ar}), 8.00 (1H, dd, J = 8.5, 2.0 Hz, H_{Ar}), 7.71 (1H, t, J = 8.5 Hz, H_{Ar}), 6.78 (1H, d, J = 8.0 Hz, H_{Ar}), 6.63 (1H, s, H_{Ar}), 6.60 (1H, dd, J = 8.0, 2.0 Hz, H_{Ar}), 3.70 (3H, s, ─OCH_3), 3.48 (2H, s, ─CH_2─), 2.07 (3H, s, ─CH_3). ^{13}C NMR (125 MHz, DMSO d_6, δ ppm): 156.1, 148.1, 146.4, 145.9, 135.1, 133.3, 130.5, 130.2, 130.0, 129.6, 128.3, 127.3, 118.5, 115.5, 112.4, 55.8, 26.5, 14.0. LC-MS (m/z) [M−H]$^-$ calcd for $C_{18}H_{16}N_3O_5$ 354.1095, found 354.1099.

4-(4-Hydroxy-3-methoxybenzyl)-3-methyl-1-(3-nitrophenyl)-1H-pyrazol-5-ol ***(4k)***: red solid, yield 87%, mp 206–208 °C. IR (ν, cm^{-1}): 3093.8 (═C─H), 1595.1 (C═C), 1514.1 and 1344.4 (NO_2). ^{1}H NMR (500 MHz, DMSO d_6, δ ppm): 11.00 (1H, brs, ─OH), 8.67 (1H, s, ─OH), 8.65 (1H, s, H_{Ar}), 8.23 (1H, d, J = 8.5 Hz, H_{Ar}), 8.02 (1H, dd, J = 8.0, 1.5 Hz, H_{Ar}), 7.72 (1H, t, J = 8.5 Hz, H_{Ar}), 6.81 (1H, s, H_{Ar}), 6.66 (1H, d, J = 8.0 Hz, H_{Ar}), 6.59 (1H, d, J = 8.0 Hz, H_{Ar}), 3.70 (3H, s, ─OCH_3), 3.52 (2H, s, ─CH_2─), 2.09 (3H, s, ─CH_3). ^{13}C NMR (125 MHz, DMSO d_6, δ ppm): 156.2, 148.1, 147.4, 144.6, 135.2, 133.3, 131.5, 130.5, 130.0, 129.2, 128.5, 120.2, 118.6, 115.4, 112.6, 55.6, 26.8, 14.1. LC-MS (m/z) [M−H]$^-$ calcd for $C_{18}H_{16}N_3O_5$ 354.1095, found 354.1099.

4-(3-Methoxybenzyl)-3-methyl-1-(3-nitrophenyl)-1H-pyrazol-5-ol ***(4l)***: red solid, yield 85%, mp 158–159 °C. IR (ν, cm^{-1}): 3076.4 (═C─H), 1604.8 (C═C), 1521.8 and 1344.4 (NO_2). ^{1}H NMR (500 MHz, DMSO d_6, δ ppm): 11.32 (1H, brs, ─OH), 8.67 (1H, s, H_{Ar}), 8.22 (1H, d, J = 7.5 Hz, H_{Ar}), 8.02 (1H, d, J = 7.5 Hz, H_{Ar}), 7.72 (1H, t, J = 8.0 Hz, H_{Ar}), 7.18 (1H, t, J = 8.0 Hz, H_{Ar}), 7.02–6.64 (3H, m, H_{Ar}), 3.71 (3H, s, ─OCH_3), 3.57 (2H, s, ─CH_2─), 2.14 (3H, s, ─CH_3). ^{13}C NMR (125 MHz, DMSO d_6, δ ppm): 157.2, 149.1, 148.1, 138.9, 138.1, 135.2, 134.3, 130.6, 130.5, 130.0, 129.3, 128.2, 127.8, 118.7, 113.1, 54.9, 26.4, 14.2. LC-MS (m/z) [M−H]$^-$ calcd for $C_{18}H_{16}N_3O_4$ 338.1146, found 338.1116.

4-(4-Methoxybenzyl)-3-methyl-1-(3-nitrophenyl)-1H-pyrazol-5-ol ***(4m)***: red solid, yield 81%, mp 198–200 °C. IR (ν, cm^{-1}): 3120.8 (═C─H), 2908.7 (C─H), 1614.4 (C═C), 1521.0 and 1322.2 (NO_2). ^{1}H NMR (500 MHz, DMSO d_6, δ ppm): 11.05 (1H, brs, ─OH), 8.67 (1H, s, H_{Ar}), 8.22 (1H, d,

J = 8.0 Hz, H_{Ar}), 8.02 (1H, dd, J = 8.5, 1.5 Hz, H_{Ar}), 7.72 (1H, t, J = 8.5 Hz, H_{Ar}), 7.14 (2H, d, J = 8.5 Hz, H_{Ar}), 6.83 (2H, d, J = 8.5 Hz, H_{Ar}), 3.70 (3H, s, —OCH_3), 3.55 (2H, s, —CH_2—), 2.08 (3H, s, —CH_3). ^{13}C NMR (125 MHz, DMSO d_6, δ ppm): 157.4, 151.2, 148.1, 139.7, 138.1, 135.0, 134.2, 130.6, 130.5, 129.2, 129.0, 118.5, 113.7, 55.0, 26.3, 14.1. LC-MS (m/z) $[M-H]^-$ calcd for $C_{18}H_{16}N_3O_4$ 338.1146, found 338.1116.

3-Methyl-4-(4-(methylthio)benzyl)-1-(3-nitrophenyl)-1H-pyrazol-5-ol ***(4n)***: red solid, yield 81%, mp 189–191 °C. IR (ν, cm^{-1}): 3198.0 (=C—H), 2918.3 (C—H), 1523.8 and 1344.4 (NO_2). ^{1}H NMR (500 MHz, DMSO d_6, δ ppm): 11.11 (1H, brs, —OH), 8.67 (1H, s, H_{Ar}), 8.21 (1H, d, J = 8.0 Hz, H_{Ar}), 8.02 (1H, dd, J = 8.0, 1.5 Hz, H_{Ar}), 7.72 (1H, t, J = 8.5 Hz, H_{Ar}), 7.20–7.16 (4H, m, H_{Ar}), 3.59 (2H, s, —CH_2—), 2.42 (3H, s, -SCH_3), 2.10 (3H, s, —CH_3). ^{13}C NMR (125 MHz, DMSO d_6, δ ppm): 155.1, 149.1, 148.1, 139.2, 138.2, 135.0, 134.3, 131.0, 130.7, 129.7, 128.1, 118.7, 113.0, 25.1, 13.6, 12.7. LC-MS (m/z) $[M-H]^-$ calcd for $C_{18}H_{16}N_3O_3S$ 354.0918, found 354.0892.

3-Methyl-4-(3-nitrobenzyl)-1-(3-nitrophenyl)-1H-pyrazol-5-ol ***(4o)***: red solid, yield 85%, mp 230–232 °C. IR (ν, cm^{-1}): 3105.4 (=C—H), 2870.1 (C—H), 1568.1 (C=C), 1523.8 and 1346.3 (NO_2). ^{1}H NMR (500 MHz, DMSO d_6, δ ppm): 10.95 (1H, brs, —OH), 8.66 (1H, s, H_{Ar}), 8.22 (1H, dd, J = 8.0, 1.0 Hz, H_{Ar}), 8.09 (1H, s, H_{Ar}), 8.06 (1H, dd, J = 8.0, 1.5 Hz, H_{Ar}), 8.03 (1H, dd, J = 8.0, 1.5 Hz, H_{Ar}), 7.75–7.71 (2H, m, H_{Ar}), 7.58 (1H, t, J = 8.0 Hz, H_{Ar}), 3.79 (2H, s, —CH_2—), 2.14 (3H, s, —CH_3). ^{13}C NMR (125 MHz, DMSO d_6, δ ppm): 157.3, 149.7, 148.1, 142.1, 142.1, 137.1, 136.2, 130.6, 130.5, 130.5, 129.1, 128.3, 127.4, 118.7, 114.9, 27.1, 14.6. LC-MS (m/z) $[M-H]^-$ calcd for $C_{17}H_{13}N_4O_5$ 353.0891, found 353.0843.

4-(Benzo[d][1,3]dioxol-5-ylmethyl)-3-methyl-1-(3-nitrophenyl)-1H-pyrazol-5-ol ***(4p)***: red solid, yield 82%, mp 170–172 °C. IR (ν, cm^{-1}): 3055.2 (=C—H), 2895.1 (C—H), 1531.5 and 1348.2 (NO_2). ^{1}H NMR (500 MHz, DMSO d_6, δ ppm): 11.15 (1H, brs, —OH), 8.67 (1H, s, H_{Ar}), 8.22 (1H, dd, J = 8.5, 1.5 Hz, H_{Ar}), 8.01 (1H, dd, J = 8.5, 2.0 Hz, H_{Ar}), 7.72 (1H, t, J = 8.0 Hz, H_{Ar}), 6.80–6.78 (2H, m, H_{Ar}), 6.69 (1H, d, J = 7.5 Hz, H_{Ar}), 5.97 (2H, s, —OCH_2O-), 3.54 (2H, s, —CH_2—), 2.10 (3H, s, —CH_3). ^{13}C NMR (125 MHz, DMSO d_6, δ ppm): 155.4, 148.2, 147.7, 145.0, 135.3, 133.2, 131.2, 130.5, 130.1, 129.7, 128.1, 120.3, 119.1, 114.8, 113.2, 102.7, 26.8, 14.1. LC-MS (m/z) $[M-H]^-$ calcd for $C_{18}H_{14}N_3O_5$ 352.0939, found 352.0911.

4-(2-Chlorobenzyl)-3-methyl-1-(4-nitrophenyl)-1H-pyrazol-5-ol ***(5a)***: yellow solid, yield 91%, mp 199–201 °C. IR (ν, cm^{-1}): 2997.8 (C—H), 1612.7 (C=C), 1532.7 and 1316.2 (NO_2). ^{1}H NMR (500 MHz, DMSO d_6, δ ppm): 11.42 (1H, brs, —OH), 8.31 (2H, d, J = 9.5 Hz, H_{Ar}), 8.05 (2H, d, J = 9.5 Hz, H_{Ar}), 7.42 (1H, dd, J = 7.5, 1.0 Hz, H_{Ar}), 7.25–7.20 (3H, m, H_{Ar}), 3.70 (2H, s, —CH_2—), 2.06 (3H, s, —CH_3). ^{13}C NMR (125 MHz, DMSO d_6, δ ppm): 155.4, 149.5, 148.1, 139.6, 138.3, 134.1, 130.8, 128.9, 128.5, 127.4, 126.5, 119.2, 113.4, 21.4, 12.6. LC-MS (m/z) $[M-H]^-$ calcd for $C_{17}H_{13}ClN_3O_3$ 342.0651, found 342.0611.

4-(2-Chloro-6-fluorobenzyl)-3-methyl-1-(4-nitrophenyl)-1H-pyrazol-5-ol ***(5b)***: yellow solid, yield 82%, mp 196–197 °C. IR (ν, cm^{-1}): 2870.1 (C—H), 1521.7 and 1327.1 (NO_2). ^{1}H NMR (500 MHz, DMSO d_6, δ ppm): 11.01 (1H, brs, —OH), 8.34 (2H, d, J = 9.0 Hz, H_{Ar}), 8.07 (2H, d, J = 9.0 Hz, H_{Ar}), 7.34–7.30 (2H, m, H_{Ar}), 7.21–7.19 (1H, m, H_{Ar}), 3.76 (2H, s, —CH_2—), 1.99 (3H, s, —CH_3). ^{13}C NMR (125 MHz, DMSO d_6, δ ppm): 160.5, 155.0, 149.3, 148.2, 139.4, 135.7, 128.8, 128.5, 124.5, 125.3, 118.8, 113.6, 113.1, 24.9, 12.5. LC-MS (m/z) $[M-H]^-$ calcd for $C_{17}H_{12}ClFN_3O_3$ 360.0557, found 360.0516.

4-(2,4-Dimethoxybenzyl)-3-methyl-1-(4-nitrophenyl)-1H-pyrazol-5-ol ***(5c)***: yellow solid, yield 89%, mp 198–200 °C. IR (ν, cm^{-1}): 2987.8 (C—H), 1521.1 and 1327.6 (NO_2). ^{1}H NMR (500 MHz, DMSO d_6, δ ppm): 10.91 (1H, brs, —OH), 8.29 (2H, d, J = 9.5 Hz, H_{Ar}), 8.04 (2H, d, J = 9.5 Hz, H_{Ar}), 6.94 (1H, d, J = 8.0 Hz, H_{Ar}), 6.51 (1H, d, J = 2.0 Hz, H_{Ar}), 6.41 (1H, dd, J = 8.5, 2.5 Hz, H_{Ar}), 3.79 (3H, s, —OCH_3), 3.70 (3H, s, —OCH_3), 3.30 (2H, s, —CH_2—), 2.06 (3H, s, —CH_3). ^{13}C NMR (125 MHz, DMSO d_6, δ ppm): 158.5, 157.9, 155.7, 149.6, 148.7, 139.8, 131.1, 128.7, 119.4, 117.3, 113.6, 106.8, 100.4, 55.9, 56.2, 25.7, 12.8. LC-MS (m/z) $[M-H]^-$ calcd for $C_{19}H_{18}N_3O_5$ 368.1252, found 368.1198.

4-(2,5-Dimethoxybenzyl)-3-methyl-1-(4-nitrophenyl)-1H-pyrazol-5-ol ***(5d)***: yellow solid, yield 89%, mp 197–198 °C. IR (ν, cm^{-1}): 2978.7 (C—H), 1511.1 and 1321.6 (NO_2). ^{1}H NMR (500 MHz, DMSO d_6, δ ppm): 10.92 (1H, brs, —OH), 8.33 (2H, d, J = 9.5 Hz, H_{Ar}), 8.08 (2H, d, J = 9.5 Hz, H_{Ar}), 6.97 (1H, d, J = 2.0 Hz, H_{Ar}), 6.53 (1H, d, J = 8.5 Hz, H_{Ar}), 6.42 (1H, dd, J = 8.5, 2.0 Hz, H_{Ar}), 3.77 (3H, s, —OCH_3), 3.69 (3H, s, —OCH_3), 3.31 (2H, s, —CH_2—), 2.08 (3H, s, —CH_3). ^{13}C NMR (125 MHz, DMSO d_6, δ ppm): 155.3, 153.6, 151.1, 149.2, 148.3, 139.5, 128.3, 127.5, 119.1, 116.6, 113.2, 112.5, 112.1, 55.7, 56.1, 26.1, 12.8. LC-MS (m/z) $[M-H]^-$ calcd for $C_{19}H_{18}N_3O_5$ 368.1252, found 368.1198.

4-(4-Methoxybenzyl)-3-methyl-1-(4-nitrophenyl)-1H-pyrazol-5-ol ***(5e)***: red solid, yield 81%, mp 209–210 °C. IR (ν, cm^{-1}): 2918.2 (C—H), 1624.1 (C=C), 1511.0 and 1312.6 (NO_2). ^{1}H NMR (500 MHz, DMSO d_6, δ ppm): 11.01 (1H, brs, —OH), 8.32 (2H, d, J = 9.0 Hz, H_{Ar}), 8.23 (2H, d, J = 9.5 Hz, H_{Ar}), 7.14 (2H, d, J = 8.5 Hz, H_{Ar}), 6.82 (2H, d, J = 8.5 Hz, H_{Ar}), 3,70 (3H, s, —OCH_3), 3.55 (2H, s, —CH_2—), 2.07 (3H, s, —CH_3). ^{13}C NMR (125 MHz, DMSO d_6, δ ppm): 156.8, 155.4, 150.2, 148.7, 140.1, 130.2, 128.8, 128.7, 118.2, 114.4, 113.5, 55.7, 25.5, 12.4. LC-MS (m/z) $[M-H]^-$ calcd for $C_{18}H_{16}N_3O_4$ 338.1146, found 338.1176.

3-Methyl-4-(4-(methylthio)benzyl)-1-(4-nitrophenyl)-1H-pyrazol-5-ol ***(5f)***: red solid, yield 90%, mp 191–193 °C. IR (ν, cm^{-1}): 2928.1 (C—H), 1521.8 and 1319.4 (NO_2). ^{1}H NMR (500 MHz, DMSO d_6, δ ppm): 11.12 (1H, brs, —OH), 8.32 (2H, d, J = 9.5 Hz, H_{Ar}), 8.07 (2H, d, J = 9.5 Hz, H_{Ar}), 7.22–7.18 (4H, m, H_{Ar}), 3.56 (2H, s, —CH_2—), 2.41 (3H, s, -SCH_3), 2.07 (3H, s, —CH_3). ^{13}C NMR (125 MHz, DMSO d_6, δ ppm): 155.1, 149.1, 148.1, 139.2, 138.2, 135.0, 134.3, 131.0, 130.7, 129.7, 128.1, 118.7, 113.0, 25.1, 13.6, 12.7. LC-MS (m/z) $[M-H]^-$ calcd for $C_{18}H_{16}N_3O_3S$ 354.0918, found 354.0903.

4-(Furan-2-ylmethyl)-3-methyl-1-(4-nitrophenyl)-1H-pyrazol-5-ol ***(5g)***: brown solid, yield 80%, mp 181–183 °C. IR (ν, cm^{-1}): 3112.3 (C—H), 1617.2 (C=N), 1521.1 (C=C). ^{1}H NMR (500 MHz, DMSO d_6, δ ppm): 10.51 (1H, brs, —OH), 8.32 (2H, d, J = 9.5 Hz, H_{Ar}), 8.07 (2H, d, J = 9.5 Hz, H_{Ar}), 8.01 (1H, d, J = 4.0 Hz, H_{Ar}), 7.26 (1H, d, J = 4.0 Hz, H_{Ar}), 6.87 (1H, dd, J = 4.0, 1.0 Hz, H_{Ar}), 3.30 (2H, s, —CH_2—), 2.06 (3H, s, —CH_3). ^{13}C NMR (125 MHz, DMSO d_6, δ ppm): 155.6, 155.0, 149.7, 148.5, 142.3, 139.8, 128.9, 119.2, 113.5, 110.5, 106.8, 25.8, 12.6. LC-MS (m/z) $[M-H]^-$ calcd for $C_{15}H_{12}N_3O_4$ 298.0833, found 298.0671.

3-Methyl-1-(4-nitrophenyl)-4-(pyridin-3-ylmethyl)-1H-pyrazol-5-ol ***(5h)***: yellow solid, yield 81%, mp 199–202 °C. IR (ν, cm^{-1}): 3120.8 (C—H), 1591.3 (C=N), 1446.8 (C=C). ^{1}H NMR (500 MHz, DMSO d_6, δ ppm): 10.81 (1H, brs, —OH), 9.35 (1H, s, H_{Ar}), 9.01 (1H, d, J = 8.0 Hz, H_{Ar}), 8.67 (1H, d, J = 4.5 Hz, H_{Ar}), 8.33 (2H, d, J = 9.5 Hz, H_{Ar}), 8.05 (2H, d, J = 9.5 Hz, H_{Ar}), 7.60–7.58 (1H, m, H_{Ar}), 3.31 (2H, s, —CH_2—), 2.08 (3H, s, —CH_3). ^{13}C NMR (125 MHz, DMSO d_6, δ ppm): 156.3, 150.7, 150.2, 149.4, 147.5, 140.7, 134.4, 132.9, 130.2, 123.6, 119.3, 114.2, 26.1, 12.9. LC-MS (m/z) $[M-H]^-$ calcd for $C_{16}H_{11}N_4O_3$ 309.0993, found 309.0988.

4.3. In vitro antibacterial and antifungal activity

The minimum inhibitory concentration of the test compounds (MIC) was determined by the micro-broth dilution technique using nutrient broth (Sheelavanth et al., 2013). All bacterial strains were maintained on nutrient agar medium at ±37 °C, and fungal strains were maintained on potato dextrose agar at ±25 °C. Serial twofold dilutions ranging from 1024 to 4 μg/mL were prepared in media. The inoculum was prepared using a 4–6 h old broth culture of each bacteria and fungi and diluted in broth media to give a final concentration of 5×10^5 CFU/mL in the test tray. The trays were covered and placed in plastic bags to prevent evaporation and are incubated at 35 °C for 18–20 h with the bacteria, and the fungal culture was incubated at 25 °C for 72 h. All determinations were done in triplicates. Ciprofloxacin and fluconazole were used as the positive control for antibacterial and antifungal activities, respectively. The MIC was defined as the lowest concentration of the compound giving complete inhibition of visible growth.

4.4. ADME-Tox predictions

The physicochemical properties were calculated using ChemBio3D (ChemBioOffice Ultra 18.0 suite). In silico prediction of the ADME properties (absorption, distribution, metabolism, and excretion) and the toxicity risks (mutagenicity, tumorigenicity, irritation, and reproduction) was performed using ADMETlab 2.0 descriptors algorithm protocol (Xiong et al., 2021) and SwissADME web tool.

4.5. In silico molecular docking studies

The structure of ligand molecules and the standards were drawn in ChemBioDraw Ultra 18.0. The energy of each molecule was minimized using ChemBio3D Ultra 18.0. The ligand molecules with minimized energy were then used as input for AutoDock Vina, in order to carry out the docking simulation. The ligand molecules with minimized energy were then used as input for AutoDock Vina, in order to carry out the docking simulation (Morris et al., 1998). Protein molecules of dihydrofolate reductase (PDB ID 4HOF and 3FYV), secreted aspartic protease (PDB ID 3Q70), *N*-myristoyl transferase (PDB ID 1IYL), gyrase B (PDB ID 4URM), thymidylate kinase (PDB ID 4QGG), and sortase A (PDB ID 2MLM) were retrieved from the protein data bank. These protein molecules were retrieved from the protein data bank. The receptors were removed all the water molecules and added only polar hydrogen and Kollman charges. The Graphical User Interface program BMGL Tools was used to set the grid box for docking simulations. The compounds or commercial drugs were docked with the target in order to determine the docking parameters with the help of Grid-based ligand docking. Auto Dock Vina was compiled and run under Windows 10.0 Professional operating system. Discovery Studio 2020 was used to deduce the pictorial representation of the interaction between the ligands and the target protein.

Declaration of Competing Interest

The authors declare that they have no known competing financial interests or personal relationships that could have appeared to influence the work reported in this paper.

Acknowledgements

The authors are thankful to the University of Medicine and Pharmacy at Ho Chi Minh City, Vietnam for granting this research (102s/2013/HĐ-NCKH).

Appendix A. Supplementary data

Supplementary data to this article can be found online at https://doi.org/10.1016/j.arabjc.2021.103682.

References

Abdel-Aziz, M., Abuo-Rahma, G.D., Hassan, A.A., 2009. Synthesis of novel pyrazole derivatives and evaluation of their antidepressant and anticonvulsant activities. Eur. J. Med. Chem. 44, 3480–3487. https://doi.org/10.1016/j.ejmech.2009.01.032.

Alam, M.M., Marella, A., Akhtar, M., Husain, A., Yar, M.S., Shaquiquzzaman, M., Tanwar, O.P., Saha, R., Khanna, S., Shafi, S., 2013. Microwave assisted one pot synthesis of some pyrazole derivatives as a safer anti-inflammatory and analgesic agents. Acta. Pol. Pharm. 70, 435–441.

Amir, M., Kumar, H., Khan, S.A., 2008. Synthesis and pharmacological evaluation of pyrazoline derivatives as new anti-inflammatory and analgesic agents. Bioorg Med. Chem. Lett. 18, 918–922. https://doi.org/10.1016/j.bmcl.2007.12.043.

Barakat, A., Al-Majid, A.M., Al-Qahtany, B.M., Ali, M., Teleb, M., Al-Agamy, M.H., Naz, S., Ul-Haq, Z., 2018. Synthesis, antimicrobial activity, pharmacophore modeling and molecular docking studies of new pyrazole-dimedone hybrid architectures. Chem. Cent. J. 12, 29. https://doi.org/10.1186/s13065-018-0399-0.

Beig, A., Agbaria, R., Dahan, A., 2013. Oral delivery of lipophilic drugs: the tradeoff between solubility increase and permeability decrease when using cyclodextrin-based formulations. PLoS ONE 8, e68237. https://doi.org/10.1371/journal.pone.0068237.

Bekhit, A.A., Ashour, H.M., Guemei, A.A., 2005. Novel pyrazole derivatives as potential promising anti-inflammatory antimicrobial agents. Arch. Pharm. (Weinheim) 338, 167–174. https://doi.org/10.1002/ardp.200400940.

Bondock, S., Rabie, R., Etman, H.A., Fadda, A.A., 2008. Synthesis and antimicrobial activity of some new heterocycles incorporating antipyrine moiety. Eur. J. Med. Chem. 43, 2122–2129. https://doi.org/10.1016/j.ejmech.2007.12.009.

Buu Hue, B.T., Kim Quy, H.T., Oh, W.K., Duy, V.D., Tram Yen, C. N., Kim Cuc, T.T., Em, P.C., Thao, T.P., Loan, T.T., Hieu, M.V., 2016. Microwave assisted synthesis and cytotoxic activity evaluations of new benzimidazole derivatives. Tetrahedron Lett. 57, 887–891. https://doi.org/10.1016/j.tetlet.2016.01.042.

Chaitannya, W.G., Virendra, R.M., Suraj, N.M., Hemchandra, K.C., Nagaiyan, S., 2019. Synthesis, bioactivities, DFT and *in-silico*

appraisal of azo clubbed benzothiazole derivatives. J Mol. Struct. 1192, 162–171. https://doi.org/10.1016/j.molstruc.2019.04.123.

Chand, K., Hiremathad, A., Singh, M., Santos, M.A., Keri, R.S., 2017. A review on antioxidant potential of bioactive heterocycle benzofuran: Natural and synthetic derivatives. Pharmacol. Rep. 69, 281–295. https://doi.org/10.1016/j.pharep.2016.11.007.

Clark, M.P., Laughlin, S.K., Laufersweiler, M.J., Bookland, R.G., Brugel, T.A., Golebiowski, A., Sabat, M.P., Townes, J.A., VanRens, J.C., Djung, J.F., Natchus, M.G., De, B., Hsieh, L.C., Xu, S.C., Walter, R.L., Mekel, M.J., Heitmeyer, S.A., Brown, K. K., Juergens, K., Taiwo, Y.O., Janusz, M.J., 2004. Development of orally bioavailable bicyclic pyrazolones as inhibitors of tumor necrosis factor-alpha production. J. Med. Chem. 47, 2724–2727. https://doi.org/10.1021/jm049968m.

Congreve, M., Carr, R., Murray, C., Jhoti, H., 2003. A 'rule of three' for fragment-based lead discovery? Drug Discov. Today. 8, 876–877. https://doi.org/10.1016/s1359-6446(03)02831-9.

El-Helby, A.A., Ayyad, R.R.A., Zayed, M.F., Abulkhair, H.S., Elkady, H., El-Adl, K., 2019. Design, synthesis, in silico ADMET profile and GABA-A docking of novel phthalazines as potent anticonvulsants. Arch. Pharm. (Weinheim) 352, e1800387. https://doi.org/10.1002/ardp.201800387.

el-Sabbagh, O.I., Baraka, M.M., Ibrahim, S.M., Pannecouque, C., Andrei, G., Snoeck, R., Balzarini, J., Rashad, A.A., 2009. Synthesis and antiviral activity of new pyrazole and thiazole derivatives. Eur. J. Med. Chem. 44, 3746–3753. https://doi.org/10.1016/j.ejmech.2009.03.038.

Em, P.C., Tuyen, T.N., Nguyen, D.H., Duy, V.D., Hong Tuoi, D.T., 2021. Synthesis of a series of novel 2-amino-5-substituted 1,3,4-oxadiazole and 1,3,4-thiadiazole derivatives as potential anticancer, antifungal and antibacterial agents. Med. Chem. 17. https://doi.org/10.2174/1573406417666210803170637.

Faidallah, H.M., Khan, K.A., Asiri, A.M., 2011. Synthesis and biological evaluation of new 3-trifluoromethylpyrazolesulfonylurea and thiourea derivatives as antidiabetic and antimicrobial agents. J. Fluor. Chem. 132, 131–137.

Galal, S.A., El-All, A.S.A., Abdallah, M.M., El-Diwani, H.I., 2009. Synthesis of potent antitumor and antiviral benzofuran derivatives. Bioorg. Med. Chem. Lett. 19, 2420. https://doi.org/10.1016/j.bmcl.2009.03.069.

Goetz, A.E., Shah, T.K., Garg, N.K., 2015. Pyridynes and indolynes as building blocks for functionalized heterocycles and natural products. Chem. Commun. (Camb) 51, 34–45. https://doi.org/10.1039/c4cc06445c.

Gokulan, P.D., Jayakar, B., Alagarsamy, V., Raja, S.V., 2012. Synthesis and pharmacological investigation of 5-substituted-3-methylsulfanyl-1*H*-pyrazole-4-carboxylic acid ethyl esters as new analgesic and anti-inflammatory agents. Arzneimittelforschung 62, 457–462. https://doi.org/10.1055/s-0032-1321830.

Güniz Küçükgüzel, S., Rollas, S., Erdeniz, H., Kiraz, M., Cevdet Ekinci, A., Vidin, A., 2000. Synthesis, characterization and pharmacological properties of some 4-arylhydrazono-2-pyrazoline-5-one derivatives obtained from heterocyclic amines. Eur. J. Med. Chem. 35, 761–771. https://doi.org/10.1016/s0223-5234(00)90179-x.

Horton, D.A., Bourne, G.T., Smythe, M.L., 2003. The combinatorial synthesis of bicyclic privileged structures or privileged substructures. Chem Rev. 103, 893–930. https://doi.org/10.1021/cr020033s.

Idrees, G.A., Aly, O.M., Abuo-Rahma, G.D., Radwan, M.F., 2009. Design, synthesis and hypolipidemic activity of novel 2-(naphthalen-2-yloxy)propionic acid derivatives as desmethyl fibrate analogs. Eur. J. Med. Chem. 44, 3973–3980. https://doi.org/10.1016/j.ejmech.2009.04.026.

Khode, S., Maddi, V., Aragade, P., Palkar, M., Ronad, P.K., Mamledesai, S., Thippeswamy, A.H., Satyanarayana, D., 2009. Synthesis and pharmacological evaluation of a novel series of 5-(substituted)aryl-3-(3-coumarinyl)-1-phenyl-2-pyrazolines as novel anti-inflammatory and analgesic agents. Eur. J. Med. Chem. 44, 1682–1688. https://doi.org/10.1016/j.ejmech.2008.09.020.

Kimata, A., Nakagawa, H., Ohyama, R., Fukuuchi, T., Ohta, S., Doh-ura, K., Suzuki, T., Miyata, N., 2007. New series of antiprion compounds: pyrazolone derivatives have the potent activity of inhibiting protease-resistant prion protein accumulation. J. Med. Chem. 50, 5053–5056. https://doi.org/10.1021/jm070688r.

Kumar, V., Kaur, K., Gupta, G.K., Sharma, A.K., 2013. Pyrazole containing natural products: synthetic preview and biological significance. Eur. J. Med. Chem. 69, 735–753. https://doi.org/10.1016/j.ejmech.2013.08.053.

Li, X., Lu, X., Xing, M., Yang, X.H., Zhao, T.T., Gong, H.B., Zhu, H.L., 2012. Synthesis, biological evaluation, and molecular docking studies of *N*,1,3-triphenyl-1*H*-pyrazole-4-carboxamide derivatives as anticancer agents. Bioorg. Med. Chem. Lett. 22, 3589–3593. https://doi.org/10.1016/j.bmcl.2012.04.066.

Lipinski, C.A., 2004. Lead- and drug-like compounds: the rule-of-five revolution. Drug Discov. Today Technol. 1, 337–341. https://doi.org/10.1016/j.ddtec.2004.11.007.

Makhija, M.T., Kasliwal, R.T., Kulkarni, V.M., Neamati, N., 2004. De novo design and synthesis of HIV-1 integrase inhibitors. Bioorg. Med. Chem. 12, 2317–2333. https://doi.org/10.1016/j.bmc.2004.02.005.

Manojkumar, P., Ravi, T.K., Subbuchettiar, G., 2009. Synthesis of coumarin heterocyclic derivatives with antioxidant activity and *in vitro* cytotoxic activity against tumour cells. Acta. Pharm. 59, 159–170. https://doi.org/10.2478/v10007-009-0018-7.

Mariappan, G., Saha, B.P., Bhuyan, N.R., Bharti, P.R., Kumar, D., 2010. Evaluation of antioxidant potential of pyrazolone derivatives. J. Adv. Pharm. Technol. Res. 1, 260–267.

Menozzi, G., Merello, L., Fossa, P., Schenone, S., Ranise, A., Mosti, L., Bondavalli, F., Loddo, R., Murgioni, C., Mascia, V., La Colla, P., Tamburini, E., 2004. Synthesis, antimicrobial activity and molecular modeling studies of halogenated 4-[1*H*-imidazol-1-yl (phenyl)methyl]-1,5-diphenyl-1*H*-pyrazoles. Bioorg. Med. Chem. 12, 5465–5483. https://doi.org/10.1016/j.bmc.2004.07.029.

Morris, G.M., Goodsell, D.S., Halliday, R.S., 1998. Automated docking using a Lamarckian genetic algorithm and an empirical binding free energy function. J. Comput. Chem. 19, 1639–1662.

Ouyang, G., Chen, Z., Cai, X.J., Song, B.A., Bhadury, P.S., Yang, S., Jin, L.H., Xue, W., Hu, D.Y., Zeng, S., 2008. Synthesis and antiviral activity of novel pyrazole derivatives containing oxime esters group. Bioorg. Med. Chem. 16, 9699–9707. https://doi.org/10.1016/j.bmc.2008.09.070.

Park, H.J., Lee, K., Park, S.J., Ahn, B., Lee, J.C., Cho, H., Lee, K.I., 2005. Identification of antitumor activity of pyrazole oxime ethers. Bioorg. Med. Chem. Lett. 15, 3307–3312. https://doi.org/10.1016/j.bmcl.2005.03.082.

Pravin, S.M., Mukesh, D.N., Vijay, K., Prakash, J., Pravin, V.B., Charansingh, H.G., 2017. An organocatalyzed efficient one-pot synthesis, biological evaluation, and molecular docking studies of 4,4′-(arylmethylene)bis-(3-methyl-1-phenyl-1*H*-pyrazol-5-ols. J. Heterocycl. Chem. 54, 1109–1120. https://doi.org/10.1002/jhet.2681.

Priego, E.M., Kuenzel, J.V.F.D., IJzerman, A.P., Camarasa, M.J., Perez-Perez, M.J., 2002. Pyrido[2,1-f]purine-2,4-dione derivatives as a novel class of highly potent human a3 adenosine receptor antagonists. J. Med. Chem. 45, 3337. https://doi.org/10.1021/jm0208469.

Ramajayam, R., Tan, K.P., Liu, H.G., Liang, P.H., 2010. Synthesis and evaluation of pyrazolone compounds as SARS-coronavirus 3C-like protease inhibitors. Bioorg. Med. Chem. 18, 7849–7854. https://doi.org/10.1016/j.bmc.2010.09.050.

Sarojini, K.B., Vidyagayatri, M., Darshanraj, G.C., Bharath, R.B., Manjunatha, H., 2010. DPPH scavenging assay of novel 1,3-disubstituted-1*H*-pyrazol-5-ols and their *in silico* studies on some proteins involved in Alzheimer's disease signaling cascade. Lett. Drug Des. Discov. 7, 214–224. https://doi.org/10.2174/157018010790596588.

Sayed, G.H., Azab, M.E., Anwer, K.E., Raouf, M.A., Negm, N.A., 2018. Pyrazole, pyrazolone and enaminonitrile pyrazole derivatives: Synthesis, characterization and potential in corrosion inhibition and antimicrobial applications. J. Mol. Liq. 252, 329–338.

Scuri, S., Petrelli, F., Grappasonni, I., Idemudia, L., Marchetti, F., Di Nicola, C., 2019. Evaluation of the antimicrobial activity of novel composite plastics containing two silver (I) additives, acyl pyrazolonate and acyl pyrazolone. Acta Biomed. 90, 370–377. https://doi.org/10.23750/abm.v90i3.8561.

Sehout, I., Boulebd, H., Boulcina, R., Nemouchi, S., Bendjeddou, L., Bramki, A., Merazig, H., Debache, A., 2021. Synthesis, crystal structure, Hirshfeld surface analysis, biological evaluation, DFT calculations, and *in silico* ADME analysis of 4-arylidene pyrazolone derivatives as promising antibacterial agents. J. Mol. Struct. 1229, 129586. https://doi.org/10.1016/j.molstruc.2020.129586.

Sheelavanth, S., Bodke, Y.D., Sundar, S.M., 2013. Synthesis, antioxidant, and antibacterial studies of phenolic esters and amides of 2-(1-benzofuran-2-yl)quinoline-4-carboxylic acid. Med. Chem. Res. 22, 1163–1171.

Sujatha, K., Shanthi, G., Selvam, N.P., Manoharan, S., Perumal, P.T., Rajendran, M., 2009. Synthesis and antiviral activity of 4,4'-(arylmethylene)bis(1*H*-pyrazol-5-ols) against peste des petits ruminant virus (PPRV). Bioorg. Med. Chem. Lett. 19, 4501–4503. https://doi.org/10.1016/j.bmcl.2009.02.113.

Thomas, R., Mary, Y.S., Resmi, K.S., Narayana, B., Sarojini, B.K., Vijayakumar, G., Van Alsenoy, C., 2019. Two neoteric pyrazole compounds as potential anti-cancer agents: Synthesis, electronic structure, physico-chemical properties and docking analysis. J. Mol. Struct. 1181, 455–466.

Venkat Ragavan, R., Vijayakumar, V., Suchetha Kumari, N., 2009. Synthesis of some novel bioactive 4-oxy/thio substituted-1*H*-pyrazol-5(4*H*)-ones via efficient cross-Claisen condensation. Eur. J. Med. Chem. 44, 3852–3857. https://doi.org/10.1016/j.ejmech.2009.04.010.

Vijesh, A.M., Isloor, A.M., Shetty, P., Sundershan, S., Fun, H.K., 2013. New pyrazole derivatives containing 1,2,4-triazoles and benzoxazoles as potent antimicrobial and analgesic agents. Eur. J. Med. Chem. 62, 410–415. https://doi.org/10.1016/j.ejmech.2012.12.057.

Xiong, G., Wu, Z., Yi, J., Fu, L., Yang, Z., Hsieh, C., Yin, M., Zeng, X., Wu, C., Lu, A., Chen, X., Hou, T., Cao, D., 2021. ADMETlab 2.0: an integrated online platform for accurate and comprehensive predictions of ADMET properties. Nucleic Acids Res. 49, W5–W14. https://doi.org/10.1093/nar/gkab255.

Xu, Z., Gao, C., Ren, Q.C., Song, X.F., Feng, L.S., Lv, Z.S., 2017. Recent advances of pyrazole-containing derivatives as anti-tubercular agents. Eur. J. Med. Chem. 139, 429–440. https://doi.org/10.1016/j.ejmech.2017.07.059.